

# Preliminary Hazard Assessment of Waste from an Advanced Fuel Cycle

NWMO-TR-2015-22

December 2015

**M. Gobien**

Nuclear Waste Management Organization

**nwmo**

NUCLEAR WASTE  
MANAGEMENT  
ORGANIZATION

SOCIÉTÉ DE GESTION  
DES DÉCHETS  
NUCLÉAIRES



**Nuclear Waste Management Organization**  
22 St. Clair Avenue East, 6<sup>th</sup> Floor  
Toronto, Ontario  
M4T 2S3  
Canada

Tel: 416-934-9814  
Web: [www.nwmo.ca](http://www.nwmo.ca)

# **Preliminary Hazard Assessment of Waste from an Advanced Fuel Cycle**

**NWMO-TR-2015-22**

December 2015

**M. Gobien**

Nuclear Waste Management Organization

**Document History**

Title:	Preliminary Hazard Assessment of Waste from an Advanced Fuel Cycle		
Report Number:	NWMO-TR-2015-22		
Revision:	R000	Date:	December 2015
Nuclear Waste Management Organization			
Authored by:	Mark Gobien		
Verified by:	Kelly Liberda		
Reviewed by:	Frank Garisto and Neale Hunt		
Approved by:	Paul Gierszewski		

**ABSTRACT**

**Title:** Preliminary Hazard Assessment of Waste from an Advanced Fuel Cycle  
**Report No.:** NWMO-TR-2015-22  
**Author(s):** Mark Gobien  
**Company:** Nuclear Waste Management Organization  
**Date:** December 2015

**Abstract**

This report documents a high-level analysis of the hazard posed by wastes generated by an advanced nuclear fuel cycle where transuranic (TRU) elements from CANDU used nuclear fuel (i.e., plutonium, neptunium, americium, and curium) are assumed to be transmuted (burned) in a fast reactor. The primary waste streams consist of fission products intentionally removed during the reprocessing process, U and TRU that enter the wastes due to inefficiencies in the reprocessing and fuel fabrication processing, and the surplus U from the fabrication of new fast reactor fuel from spent CANDU fuel. The inventories in the waste stream from a fast reactor based fuel cycle were previously estimated using mass balance calculations.

This report considers pyroprocessing as the reference method used to reprocess spent CANDU and spent fast reactor fuel. The waste salt from pyroprocessing is assumed to be converted into a stable ceramic-glass wasteform. The properties and radionuclide loading of the fast reactor wasteform used to encapsulate waste stream radionuclides extracted during reprocessing are described based on available literature.

With respect to the hazard of the fast reactor wasteform, the wasteform radioactivity, radiotoxicity, thermal power, and unshielded dose rate are estimated and compared to an equivalent amount of spent CANDU fuel. This analysis shows that the fast reactor wasteform from reprocessing and spent CANDU fuel are broadly similar on a per kg of wasteform basis. The fast reactor wasteform is more hazardous in the short term, and the spent CANDU fuel is more hazardous in the long term.

Finally, the long-term safety of the fast reactor waste is considered. Two options are considered - placement in a deep geological repository, and placement after 300-years decay in a near-surface landfill. This analysis shows that the dose consequences as a result of surface disposal of reprocessing wastes would be high over long periods of time. That is, even after several hundred years of decay, the fast reactor wasteform is a long-lived nuclear waste which would require appropriate management such as a deep geological repository.



**TABLE OF CONTENTS**

		<b><u>Page</u></b>
<b>ABSTRACT</b>	.....	<b>iii</b>
<b>1.</b>	<b>INTRODUCTION</b> .....	<b>1</b>
<b>2.</b>	<b>KEY ASSUMPTIONS</b> .....	<b>1</b>
<b>2.1</b>	<b>NUCLEAR FUEL CYCLE</b> .....	<b>1</b>
<b>2.2</b>	<b>REPROCESSING</b> .....	<b>3</b>
<b>2.3</b>	<b>REPROCESSING WASTES AND WASTEFORM</b> .....	<b>4</b>
2.3.1	Wasteform .....	4
2.3.2	Fission Products .....	6
2.3.3	Uranium and TRUs .....	6
2.3.4	Light Element Activation Products .....	6
2.3.5	Other Wastes .....	6
<b>2.4</b>	<b>WASTE INVENTORY</b> .....	<b>7</b>
<b>3.</b>	<b>NATURE OF THE HAZARD</b> .....	<b>8</b>
<b>3.1</b>	<b>WASTE RADIOACTIVITY</b> .....	<b>9</b>
<b>3.2</b>	<b>WASTE RADIOTOXICITY</b> .....	<b>11</b>
<b>3.3</b>	<b>WASTE THERMAL POWER</b> .....	<b>13</b>
<b>4.</b>	<b>UNSHIELDED DOSE ASSESSMENT</b> .....	<b>15</b>
<b>4.1</b>	<b>MODELLING PARAMETERS</b> .....	<b>15</b>
4.1.1	Dimensions .....	15
4.1.2	Composition of Materials .....	15
4.1.3	Source Activity .....	16
4.1.4	Buildup Factor .....	16
4.1.5	Integration Parameters .....	16
<b>4.2</b>	<b>DOSE RESULTS</b> .....	<b>16</b>
<b>5.</b>	<b>POSTCLOSURE SAFETY</b> .....	<b>18</b>
<b>5.1</b>	<b>DEEP GEOLOGICAL REPOSITORY</b> .....	<b>18</b>
<b>5.2</b>	<b>SURFACE DISPOSAL (LANDFILL) ASSESSMENT</b> .....	<b>19</b>
5.2.1	Conceptual Model .....	20
5.2.2	Assessment Data .....	21
5.2.2.1	Radionuclide Inventory and Half-Lives .....	21
5.2.2.2	Release Rate from the Fast Reactor Wasteform .....	22
5.2.2.3	Solubility Limits .....	24
5.2.2.4	Landfill Transport Properties .....	24
5.2.2.5	Aquifer and Well Properties .....	24
5.2.2.6	Dose Pathway Data .....	25
5.2.3	Dose Results .....	25
<b>6.</b>	<b>SUMMARY</b> .....	<b>27</b>
<b>REFERENCES</b>	.....	<b>29</b>
<b>APPENDIX A – WASTE PROFILES FOR SPENT CANDU FUEL</b>	.....	<b>33</b>

<b>APPENDIX B – AMBER MODEL THEORY .....</b>	<b>41</b>
<b>B.1 COMPARTMENT MODELLING.....</b>	<b>41</b>
<b>B.2 WASTEFORM DEGRADATION .....</b>	<b>41</b>
<b>B.3 ADVECTIVE AND DIFFUSIVE TRANSPORT .....</b>	<b>41</b>
<b>B.4 DOSE PATHWAYS.....</b>	<b>42</b>

**LIST OF TABLES**

	<b><u>Page</u></b>
Table 1: System Inventory for 36 Fast Reactors and 103,000 t <sub>HM</sub> CANDU Used Fuel .....	7
Table 2: Composition of Zeolite (Ugal et al. 2010).....	15
Table 3: Composition of Borosilicate Glass (Corning, 2015) .....	15
Table 4: Dominant Waste Products (Tait et al. 2000) .....	16
Table 5: Composition of Waste Salt (Priebe and Bateman, 2006) .....	16
Table 6: Normalized Release Rates [kg/m <sup>2</sup> /a] .....	23
Table 7: Landfill Transport Properties .....	24
Table 8: Summary of the Long-Term Characteristics of the Total CANDU and Fast Reactor Wastes .....	28

**LIST OF FIGURES**

	<b><u>Page</u></b>
Figure 1: Nuclear Fuel Cycle Considered in Analysis .....	2
Figure 2: Pyroprocessing Cycle for Oxide and Metallic Used Fuel (ANL, 2012).....	3
Figure 3: Ceramic Waste Process (Simpson, 2012).....	5
Figure 4: Glass-Bonded Zeolite Wasteform (Phongikaroon, 2014) .....	5
Figure 5: Fast Reactor Wasteform Radioactivity .....	9
Figure 6: CANDU Fuel Radioactivity.....	10
Figure 7: Total Radioactivity for All CANDU Fuel, Fast Reactor Wasteforms and Surplus Uranium .....	10
Figure 8: Fast Reactor Wasteform Radiotoxicity .....	11
Figure 9: CANDU Fuel Radiotoxicity.....	12
Figure 10: Total Radiotoxicity for All CANDU Fuel, Fast Reactor Wasteforms, and Surplus Uranium .....	12
Figure 11: Thermal Power of a Fast Reactor Wasteform .....	13
Figure 12: Thermal Power of CANDU Fuel.....	14
Figure 13: Total Thermal Power for All CANDU Fuel, Fast Reactor Wasteforms and Surplus Uranium .....	14
Figure 14: Dose Rate from the Fast Reactor Wasteform as a Function of Decay Time and Distance .....	17
Figure 15: Annual Dose Rate at 10 m from a Fast Reactor Wasteform and a CANDU Fuel Bundle per Unit Mass .....	17
Figure 16: Generic Design Option II - Double Composite Liner.....	20
Figure 17: Conceptual AMBER Model .....	21
Figure 18: Effect of Wasteform Degradation Model on Dose Rate as a Function of Time for a Delay of 300a.....	26
Figure 19: Effect of Model Assumptions on Dose Rate as a Function of Time.....	26



## 1. INTRODUCTION

Ion (2015) provides an assessment of the implications of adopting an advanced fuel cycle where used CANDU fuel is reprocessed and supplied to fast reactors designed to burn actinides. The fuel cycle specifically incorporates fuel reprocessing and recycling to separate actinides including plutonium from used fuel, for use as the new fuel source. Ion (2015) quantifies the extent to which such a program would result in a shift of the high-level waste towards less TRansUranic (TRU) waste and more fission product wastes.

The purpose of this work is to estimate the implications of the waste from this fast reactor based fuel cycle on the following, compared to a once-through CANDU fuel cycle:

- radioactivity as a function of time;
- radiotoxicity as a function of time;
- thermal power as a function of time;
- dose to an unshielded person as a function of distance; and
- comparison of disposal in a deep geological repository versus a surface facility (landfill).

Understanding the long-term hazard of the wastes from an advanced fuel cycle is important to assess options for their long-term management. The following analysis is a preliminary estimate based on literature information and simple models.

## 2. KEY ASSUMPTIONS

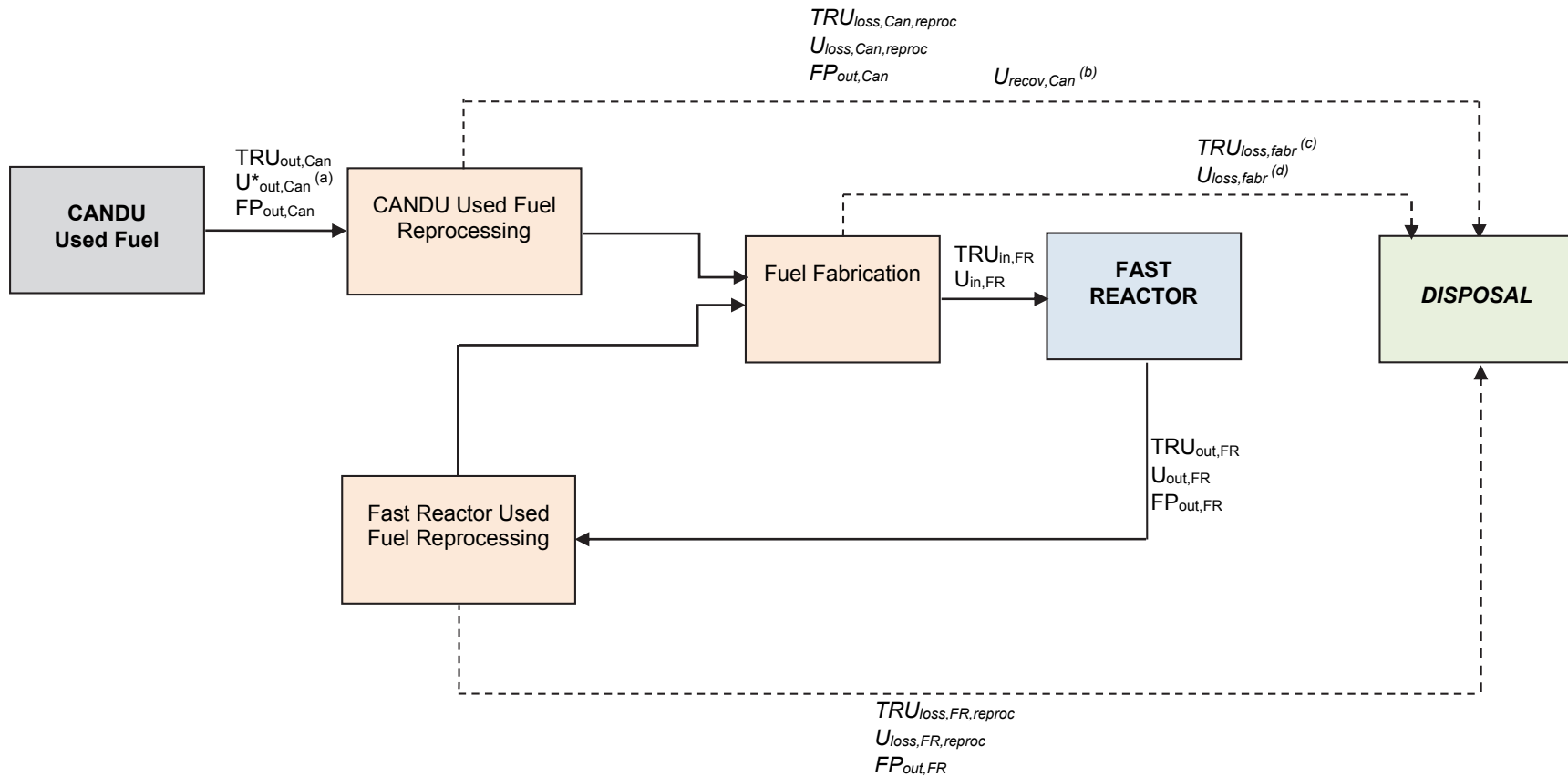
### 2.1 NUCLEAR FUEL CYCLE

A closed nuclear fuel cycle utilizing fast reactors is illustrated in Figure 1 (Ion, 2015). Fast reactors can be theoretically operated as either “breeders” or “burners”, depending on the conversion ratio<sup>1</sup>. A “breeder” fast reactor is attractive in that it makes its own fuel once started, i.e., it can convert ordinary uranium into useful fissile fuel. Historically, this has been the focus of many fast reactor programs. In contrast, a “burner” fast reactor requires a continuous external source of fissile material in addition to uranium, and the external fuel could include plutonium and TRUs from used thermal reactor fuel. In this mode, therefore, burner fast reactors have been proposed for waste management purposes.

In this analysis it is assumed that used CANDU fuel is reprocessed to recover the uranium, plutonium and other actinides, which are then used to fabricate the fresh fuel required for starting and operating a fleet of burner fast reactors. Once in operation, the used fast reactor fuel is reprocessed and recycled continuously together with makeup from used CANDU fuel to produce energy.

---

<sup>1</sup> “Conversion (breeding) ratio” is defined as the number of fissionable atoms produced to the number of fissionable atoms consumed in a reactor. If the ratio is less than 1, it is referred to as “conversion ratio”. If it is greater or equal to 1, it is referred to as “breeding ratio”. (Cacuci 2010, Sec.1.5.)



**Notes:**

- $U_{out,Can}^{*}$  is the total amount of uranium available in CANDU used fuel, out of which a smaller quantity ( $U_{out,Can}$ ) is used for reprocessing and for fabrication of the fast reactor fuel.
- $U_{recov,Can}$  is the amount of uranium recovered from reprocessing of CANDU used fuel, and not used for fabrication of the fast reactor fuel, which could be either stored for future re-use as make-up in the fast reactor or sent for disposal.
- $TRU_{loss, fabr}$  represents the total TRU losses from fast reactor fuel fabrication using reprocessed CANDU and fast reactor used fuels.
- $U_{loss, fabr}$  represents the total U losses from fast reactor fuel fabrication using reprocessed CANDU and fast reactor used fuels.

**Figure 1: Nuclear Fuel Cycle Considered in Analysis**

Note that in the reference fuel cycle analysis presented in Ion (2015), the TRU content is considered as an aggregate, without specifically focussing on the isotopic content. The TRU includes the total plutonium, neptunium, americium, and curium content of the fuel. In practice, a certain amount of more fissile isotopes would be required in the fast reactor core. The analysis documented in Ion (2015) therefore is optimistic with respect to its ability to transmute TRUs from used CANDU fuel. It may be that an additional supply of some isotopes would be needed, in order to make the reactor physics work.

## 2.2 REPROCESSING

Reprocessing is a key process in a closed fuel cycle. Various technologies are presently being considered, notably aqueous, pyro, and fluoride volatility processes. The reprocessing technology considered in this analysis for both CANDU and fast reactor used fuel is 'pyroprocessing'.

The key processes involved in the pyroprocessing of used fuel include fuel chopping, electrorefining and cathode processing as illustrated in Figure 2. Electrorefining is the key operation, this process removes waste fission products from the uranium, plutonium and other actinides in the used fuel. Electrorefining is very similar to electroplating. Used fuel attached to an anode and suspended in a chemical bath (typically molten chloride salt), and an electric current then dissolves the used fuel and plates out the uranium, plutonium and other actinides on a cathode. These extracted elements are then sent to the cathode processor where the residual salt from the refining process is removed.

For oxide fuels, an additional step is required prior to the electrorefining process. This step involves reducing the oxide fuel to a metallic form so the used fuel is suitable for electrorefining. Early research into the oxide reduction process focussed on chemical reduction using lithium metal dissolved in LiCl (Karell et al., 2001), whereas the emphasis in the last decade has been on electrolytic reduction using LiCl-Li<sub>2</sub>O as the electrolyte (Simpson, 2012).

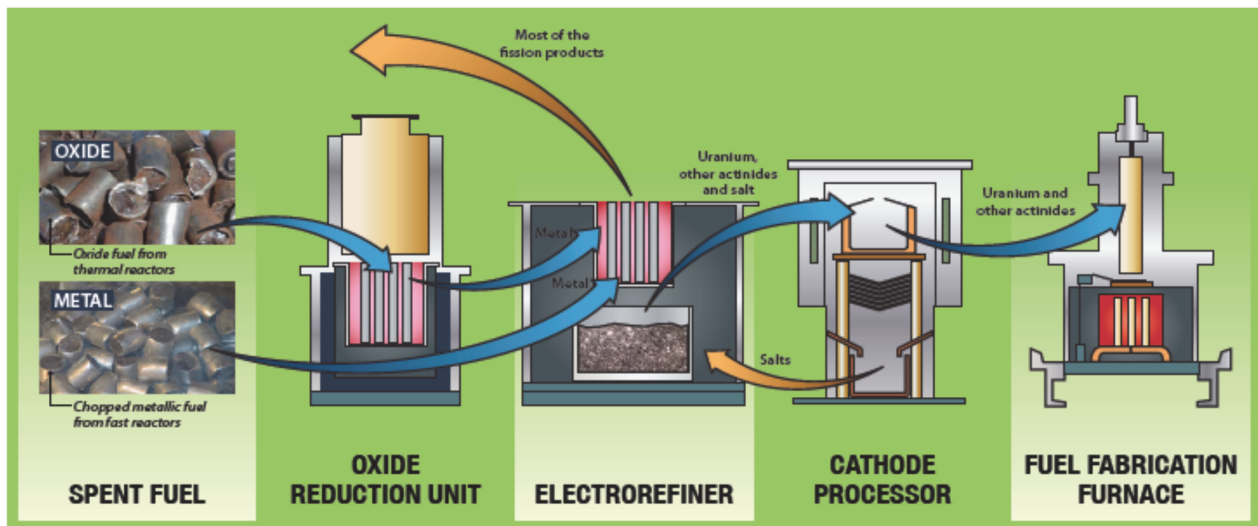


Figure 2: Pyroprocessing Cycle for Oxide and Metallic Used Fuel (ANL, 2012)

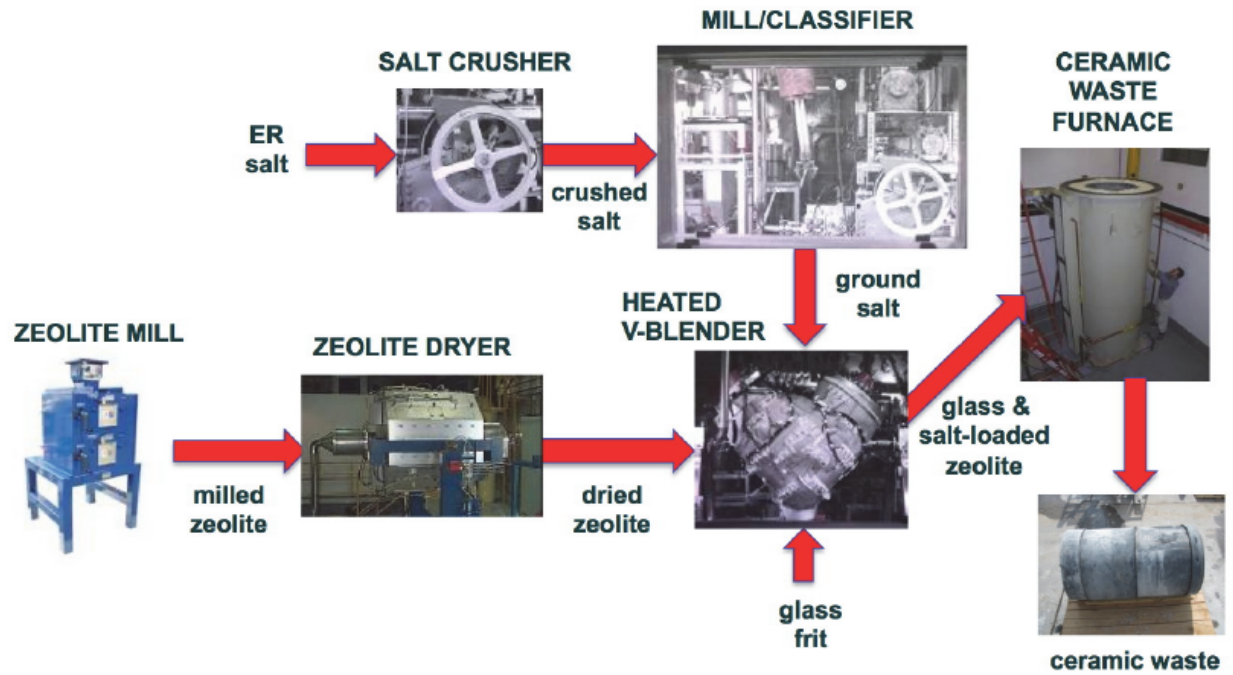
Pyroprocessing of used EBR (Experimental Breeder Reactor) II fast reactor fuel has been successfully carried out on a small scale (Simpson, 2012). Pyroprocessing of used CANDU fuel has not been demonstrated. However, laboratory scale tests of reprocessing used light water reactor fuel, a uranium rich oxide fuel, have been successfully completed (Herrmann et al., 2006). The present analysis assumes that pyroprocessing can be successfully adopted to reprocess used CANDU fuel as well as used fast reactor fuels on a commercial scale (see Ion 2015 for estimates of the reprocessing rates needed).

## **2.3 REPROCESSING WASTES AND WASTEFORM**

### **2.3.1 Wasteform**

Waste salt from the electrorefining process must be transformed into a stable, non-soluble, wasteform for disposal. Borosilicate glass has been used as a medium to solidify high-level waste from aqueous processing; however it has a low capacity for chloride ions (Kim et al., 2007). Therefore a ceramic waste process (Simpson, 2012) is adopted as the reference process for preparing waste salt for disposal. The fast reactor wasteform is comprised of three primary components including 7-15 wt% salt wastes and radionuclides from the electrorefiner 60-68 wt% zeolite (a crystalline aluminosilicate material that has a high capacity for adsorption of various molecular species), and 25 wt% borosilicate glass (Kim et al., 2007). The zeolite-to-waste-salt ratio is somewhat variable, with some reports having successfully created wasteforms with waste salt loading as high as 20 wt% (Pereira and Babcock, 1996) while other sources found a zeolite to salt ratio of 9 to be optimal for ceramic waste manufacturing (Nagarajan et al., 2010). The exact ratio of zeolite to salt will depend on the type of zeolite used and the ceramic waste fabrication procedure.

The ceramic waste process consists of several unit operations, including zeolite size reduction, zeolite drying, salt/zeolite blending, and pressureless consolidation. Figure 3 shows a detailed schematic of the ceramic waste process. The objective of the ceramic waste process is to immobilize the salt containing fission products and other radioactive species into glass-bonded zeolite ingots with a nominal mass of 400 kg, density of 1870 kg/m<sup>3</sup>, radius of 0.35 m and a height of 0.556 m (Priebe and Bateman, 2006). Figure 4 shows a sample of a glass-bonded zeolite wasteforms produced at the Idaho National Laboratory.



Note: Waste salt ion exchange is not shown

**Figure 3: Ceramic Waste Process (Simpson, 2012)**

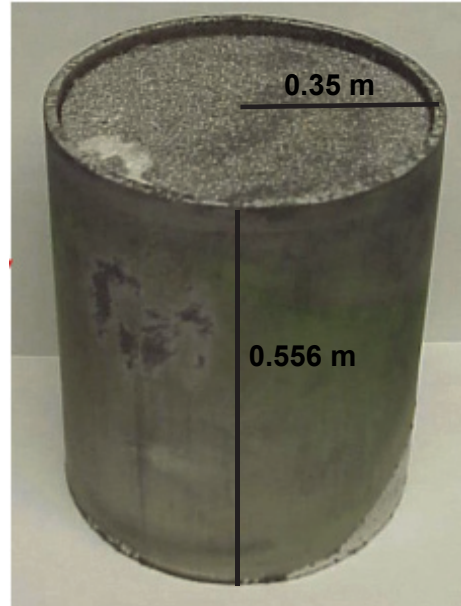


**Figure 4: Glass-Bonded Zeolite Wasteform (Phongikaroon, 2014)**

### 2.3.2 Fission Products

It is assumed that all fission products in the used fuel are contained in the waste salts, including all volatile fission products, and sent for disposal.

Prior to encapsulating the electrorefiner salts in a wasteform, the fission products can be concentrated in the zeolite using an ion-exchange column. Pereira and Babcock (1996) show that for waste salt with an initial fission product weight fraction of 7.0%, hot blending with zeolite yields a fission product concentration of 1.75 wt% in the wasteform, and utilizing an ion exchange process generates a final fission product loading of 8 wt% in the final wasteform. This assessment will assume the waste salts go through an ion exchange process to reduce the final volume of wastes and the resulting wasteform will contain 8 wt% fission products.

### 2.3.3 Uranium and TRUs

Theoretical pyroprocessing flowsheets have been developed to estimate the material balances for recycling actinides from the light water reactor spent fuel for use in fast reactors (OECD 2012, Williamson and Willit 2011, Berger and Benedict 2011, Yoo et al. 2008). The efficiencies assumed for the recovery of the actinides are typically within 99.0 – 99.9 wt% (OECD 2012, Yoo et al. 2008, Nuclear Fuel Cycle Options Catalog 2014). Some studies assume a very high efficiency, such as 99.9%, which would maximize the amount of actinides recovered from pyroprocessing (OECD 2012, Sec. 2.4; Williamson and Willit 2011, Sec. 2). Others explore the implications of using different recovery efficiencies for the TRU and U streams, for example, 97 wt% efficiency for TRU recovery and 98 wt% for uranium, based on experimental results and technical information available in the open literature (Yoo et al. 2008). Lee and Kim (2015) recently reported results of a case study assuming different TRU recovery efficiencies (i.e., 99.9 – 99.9999 wt%) for recycling TRUs from CANDU used fuel for use in fast reactors.

The present analysis assumes 100 wt% recovery of fission products, 99.5 wt% for recovery of TRU elements and 99.0 wt% for the recovery of uranium, during fuel reprocessing. Note that this is an overall efficiency; the analysis does not consider the efficiencies associated with each individual step of the reprocessing technology.

The overall fabrication efficiency for TRU elements and uranium during fuel fabrication is assumed to be 99.9 wt%.

### 2.3.4 Light Element Activation Products

Spent CANDU fuel and fast reactor fuel will also contain small amounts of light element activation products from impurities in the fuel (Tait et al. 2000), most notably C-14. This analysis will assume all the light element activation products from the reprocessed CANDU and fast reactor fuel are encapsulated in the fast reactor wasteform.

### 2.3.5 Other Wastes

After each fuel batch is electrorefined, the fuel sheaths remain in the anode baskets along with unreacted actinides, zirconium, noble metals, and residual waste salt. It has been shown that zirconium and noble metal retention is a function of the extent of actinide removal; however, most of these elements tend to be retained with the cladding hulls (Li and Simpson, 2005). A metal waste furnace would be used to consolidate the cladding hulls and residual fuel constituents into a metallic ingot (Simpson, 2012). Wastes from the cladding hulls are not considered in this analysis.

Other low and intermediate level wastes generated during the operation of the reprocessing facility are also not considered in this analysis.

## 2.4 WASTE INVENTORY

Calculations in Ion (2015) show that if 36 fast reactors were put into operation, with an optimistic conversion ratio of 0.25, to replace the existing Canadian nuclear reactor fleet, it would take just over 40 years to burn about 80% of the TRUs in the 103,000 t<sub>HM</sub> (tonnes heavy metals) of CANDU used fuel (Garamszeghy, 2014). The remainder of the TRUs would be within the fast reactor fuel at shutdown, and would either require disposal or consumption in the continued operation of a smaller number of fast reactors.

Reprocessing of the CANDU used fuel and the fast reactor used fuel will generate a significant amount of waste products that will need to be disposed of. Table 1 from Ion (2015) shows estimates of the total mass of fission products, U and TRU sent for disposal.

**Table 1: System Inventory for 36 Fast Reactors and 103,000 t<sub>HM</sub> CANDU Used Fuel**

Source		Initial	Final <sup>1</sup>
Unreprocessed CANDU Used Fuel [t]	U	101,524	714.4
	TRU	454	3.2
	FP	1022	7.2
Fast Reactor Core(s) [t]	U	0	93.3
	TRU	0	112.8
	FP	0	16
Reprocessing and Fuel Fabrication:			
Waste Sent for Disposal [t]	U <sup>2</sup>	0	1018.5
	TRU <sup>2</sup>	0	8.7
	FP	0	1485.8
Uranium Recovered from Reprocessing of CANDU Used Fuel Stored for Re-use or Sent for Disposal [t]	U	0	99,540.2
Total U [t]		101,524	101,366
Total TRU [t]		454	125
Total FP [t]		1022	1509

Notes:

- 1) At the end of year 41, there will be insufficient TRU in the unprocessed CANDU used fuel to continue operation of the fast reactors with a conversion ratio of 0.25.
- 2) U and TRU losses during reprocessing and fuel fabrication of CANDU and fast reactor used fuel, sent with the FP for disposal.

Ion (2015) estimates that, for this scenario, roughly 1486 tonnes of fission products, 1019 tonnes of U and 8.7 tonnes of TRUs will be sent for disposal. Assuming the 400 kg fast reactor

wasteform (see Section 2.3.1) contains roughly 8 wt% (32 kg) of waste products (Pereira and Babcock, 1996) results in 78,553 waste packages (each with one 400-kg wasteform). This would mean 31,421 tonnes of waste, about one third of the initial 101,524 tonnes of used CANDU fuel. Assuming the fission products, U and TRU wastes are evenly distributed amongst all the waste packages means each package will contain roughly 18.9 kg of fission products, 13 kg of U and 0.11 kg of TRU.

Ion (2015) does not consider the light element activation products produced in irradiated fuel (such as C-14 from activation of trace levels of N in the fuel). For the reference scenario with 103,000  $t_{HM}$  used CANDU fuel, the calculations in Ion (2015) shows that the fission products from reprocessed CANDU fuel makes up roughly two thirds of the total waste inventory. The total inventory of radioactive light element activation products from reprocessed CANDU fuel is 501 kg (Tait et al. 2000); the proportional amount in the fast reactor fuel is estimated to be 251 kg. Assuming all these activation products are evenly distributed amongst the 78,553 waste packages results in each waste package containing approximately 0.0096 kg of light element activation products.

One also has to consider the radionuclide makeup of fission products, U, TRUs and light element activation products present in the fast reactor wasteform. For this analysis the reference radionuclide makeup is assumed to be that of CANDU used fuel with a burnup of 220 MWh/kgU (Tait et al., 2000). That is, the amount of a radionuclide per kg of fission products would be the same as in CANDU fuel. This is reasonable because roughly two thirds of fission products and nearly all the uranium, which make up the bulk of the radionuclides in the waste stream, are from the reprocessing of spent CANDU fuel (Ion, 2015). The radionuclide profile in fast reactor used fuel will be different because of the different initial fuel composition, different neutron spectrum, and the higher fuel burnup. However, a relevant fission product inventory data for spent fast reactor fuel for this scenario is not currently available.

Appendix A lists the initial inventory (in kg) of radionuclides used in this analysis.

It should be noted that the 99,540 tonnes of uranium recovered from reprocessing for reuse or disposal are assumed to be reused and are not included in the fast reactor wasteform described above. The consequences of this excess uranium are largely not considered in this analysis. However, for comparison, the radioactivity, radiotoxicity and thermal power of the excess uranium is compared to the total radioactivity, radiotoxicity and thermal power of the 5.2 million CANDU fuel bundles and 78,553 fast reactor wasteforms in sections 3.1 through 3.2.

Additionally, the significant amount of TRUs and FPs remaining in the 36 fast reactor cores at the end of this scenario is not included in the analysis below. This analysis also does not include the approximately 12,000 tonnes of radioactive zirconium alloy recovered from the used CANDU fuel. It is assumed that this is reused in fabricating the fast reactor fuel, and its ultimate disposal is not considered here.

### **3. NATURE OF THE HAZARD**

The following analysis considers the hazard of the waste product from the fast reactor fuel cycle. It does not consider the remaining unprocessed CANDU used fuel, nor the remaining radioactivity in the fast reactor cores.

### 3.1 WASTE RADIOACTIVITY

Figure 5 and Figure 6 show that calculated radioactivity as a function of time for the fast reactor wasteform and for CANDU fuel respectively. For comparison, the radioactivity is presented in  $\text{Bq/kg}_{\text{wasteform}}$ , this means that the total radioactivity of the wasteform is divided by the total mass of fast reactor wasteform (400 kg) and the CANDU fuel (24 kg). Note that the total radioactivity of the CANDU fuel does not include the contribution made by the Zircaloy, and time zero corresponds to the time of discharge from the reactor.

Figure 5 shows the radioactivity in the fast reactor wasteform is completely dominated by the contribution from the fission products. The fission product radioactivity is dominated by Cs-137 and Sr-90 and their daughters Ba-137m and Y-90 for the first 300 years after discharge. Between 300 and 1,000,000 years the radioactivity is dominated by Tc-99 and beyond 1,000,000 year the radioactivity is controlled by Zr-93 and Nb-93m. Figure 6 shows the radioactivity of the CANDU fuel is initially controlled by the fission products with actinides (namely Am-241, Pu-240, Pu-239 and eventually Bi-210 and Po-210) becoming the dominant source of radioactivity after a few hundred years. Due to the higher fission product loading in the fast reactor wasteform, the initial radioactivity is approximately 1.5 times higher than the CANDU fuel, but after a few hundred years the radioactivity of the CANDU fuel is higher than the fast reactor wasteform. Figure 7 compares the total radioactivity of the entire inventory of fast reactor wasteforms, CANDU fuel and surplus uranium.

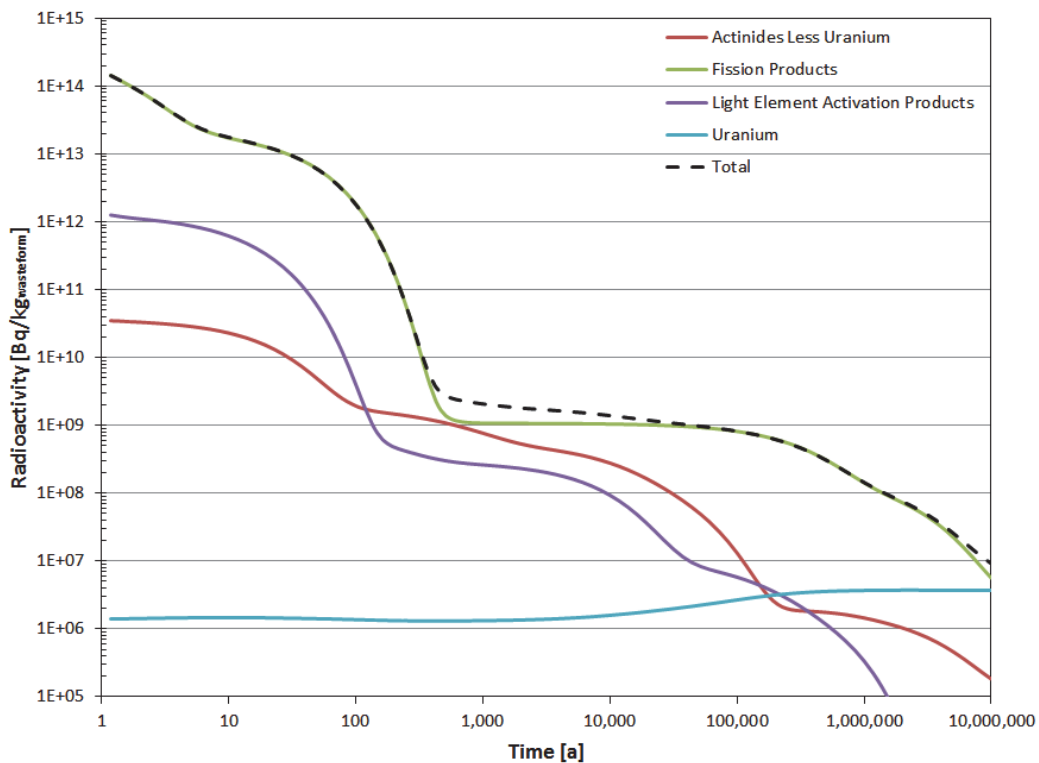


**Figure 5: Fast Reactor Wasteform Radioactivity**

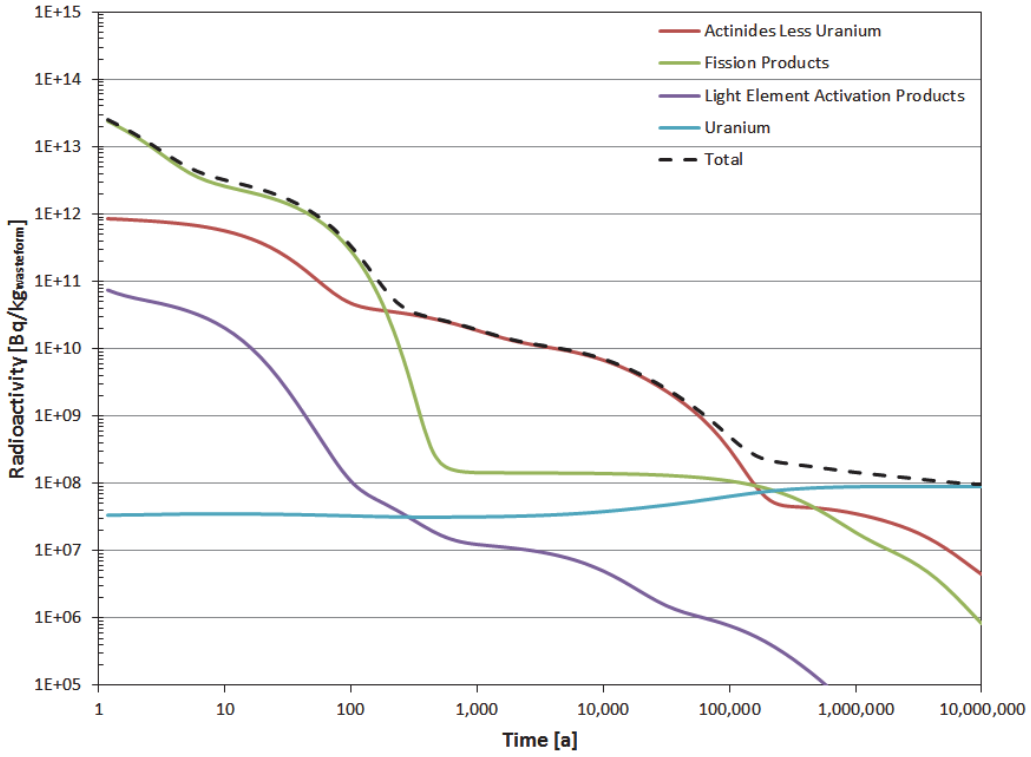


Figure 6: CANDU Fuel Radioactivity

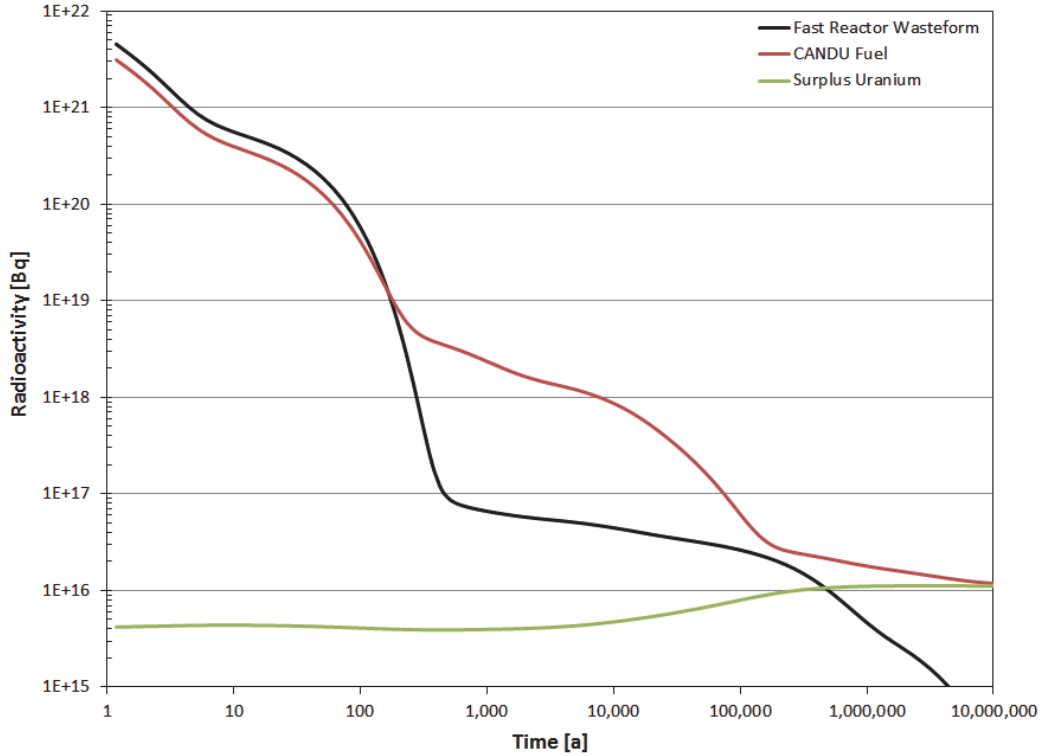
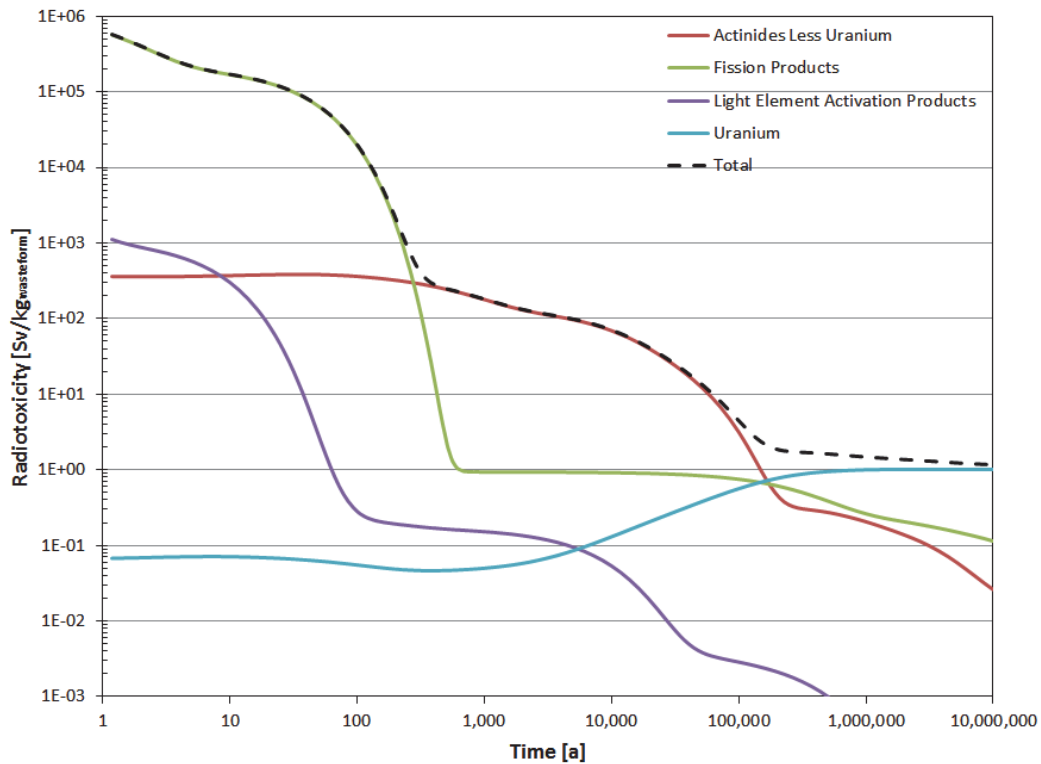


Figure 7: Total Radioactivity for All CANDU Fuel, Fast Reactor Wasteforms and Surplus Uranium

### 3.2 WASTE RADIOTOXICITY

Figure 8 and Figure 9 show the ingestion radiotoxicity (in  $\text{Sv}/\text{kg}_{\text{wasteform}}$ ) of the fast reactor wasteform and CANDU fuel respectively. The radiotoxicity was calculated by multiplying the radioactivity of each radionuclide (in  $\text{Bq}/\text{kg}_{\text{wasteform}}$ ) by that radionuclide's corresponding ingestion dose coefficient in  $\text{Sv}/\text{Bq}$  (ICRP, 1996, Gobien and Garisto, 2012). Figure 8 shows the radiotoxicity of the fast reactor wasteform is dominated by the fission products at early times and then the actinides at later times. The first few hundred years are dominated by Sr-90 and Cs-137 while Am-241, Pu-239 and Pu-240 dominate between 1,000 and 300,000 years. The uranium daughters (notably Po-210) control the radiotoxicity beyond 300,000 years. The radiotoxicity of the CANDU fuel (Figure 9) follows a similar trend with fission products (Sr-90 and Cs-137) initially controlling the radiotoxicity and actinides (Am-241, Pu-239, Pu-240 and Po-210) dominating after a few hundred years. The larger actinide inventory in the CANDU fuel results in a higher overall radiotoxicity beyond a few hundred years and after 1,000,000 years the CANDU fuel is approximately 20 times more radiotoxic than the fast reactor wasteform.

Figure 10 compares the radiotoxicity of the entire inventory of fast reactor wasteforms, CANDU fuel and surplus uranium. Figure 10 is a reminder that the long-term management of the separated uranium is a factor that needs to be considered in evaluation of future scenarios.



**Figure 8: Fast Reactor Wasteform Radiotoxicity**

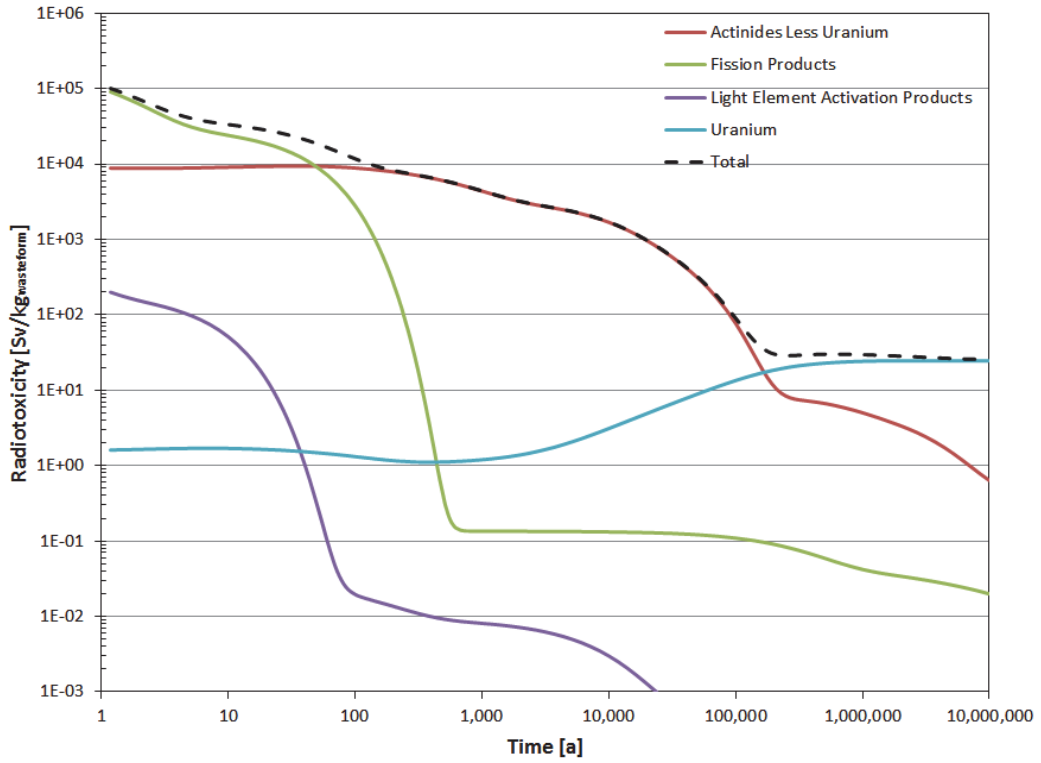


Figure 9: CANDU Fuel Radiotoxicity

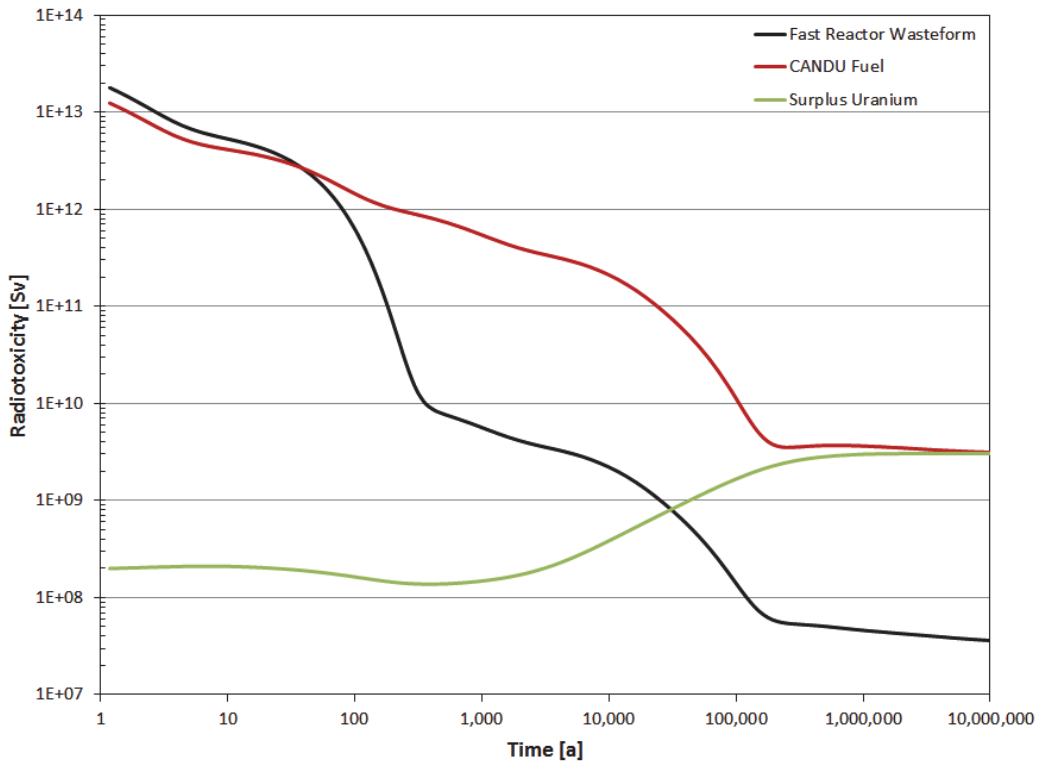


Figure 10: Total Radiotoxicity for All CANDU Fuel, Fast Reactor Wasteforms, and Surplus Uranium

### 3.3 WASTE THERMAL POWER

Figure 11 and Figure 12 show the thermal power (in  $\text{W}/\text{kg}_{\text{wasteform}}$ ) for the fast reactor wasteform and CANDU fuel respectively. The thermal power was calculated using the radionuclide thermal power (in  $\text{W}/\text{kg}$ ) from Tait et al. (2000) for the spent CANDU fuel. For the fast reactor wasteform the thermal power from Tait et al. (2000) were also used but scaled relative to the fast reactor wasteform inventory. Similar to the radiotoxicity, Figure 11 shows the thermal power of the fast reactor wasteform is initially dominated by fission products (Sr-90 and Cs-137) followed by actinides (Am-241, Pu-239, Pu-240 and uranium daughters) at later times. Unlike the radiotoxicity, Tc-99 briefly dominates the thermal power after a few hundred thousand years before the uranium daughters take over. Figure 12 shows the thermal power of the CANDU fuel is initially dominated by the same fission products (Sr-90 and Cs-137) for a brief period of time and then by the actinides (Am-241, Pu-240, Pu-239 and Po-210) for the remaining time. Relative to the CANDU fuel, the fast reactor wasteform initially has a higher thermal power per unit mass but over time this decreases to a level below that of the CANDU fuel (Figure 13).

The surplus uranium is also shown in Figure 13. It initially has a much lower thermal power than the CANDU fuel and fast reactor wasteform but eventually increases to a level equal to the CANDU fuel at long times.

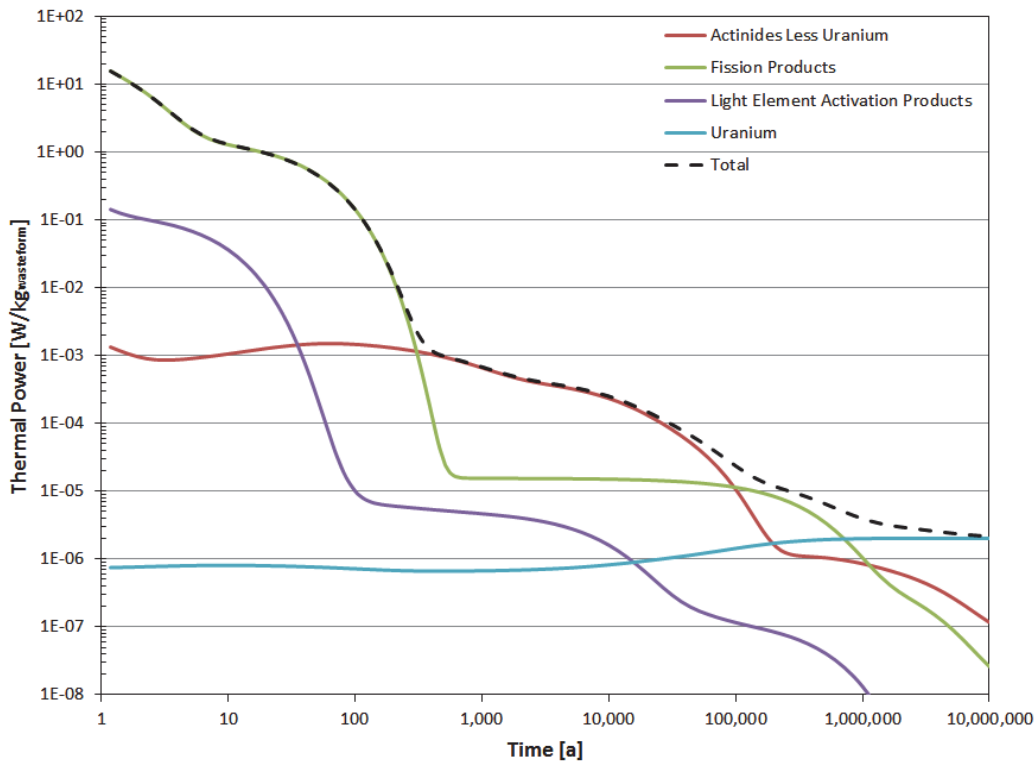


Figure 11: Thermal Power of a Fast Reactor Wasteform

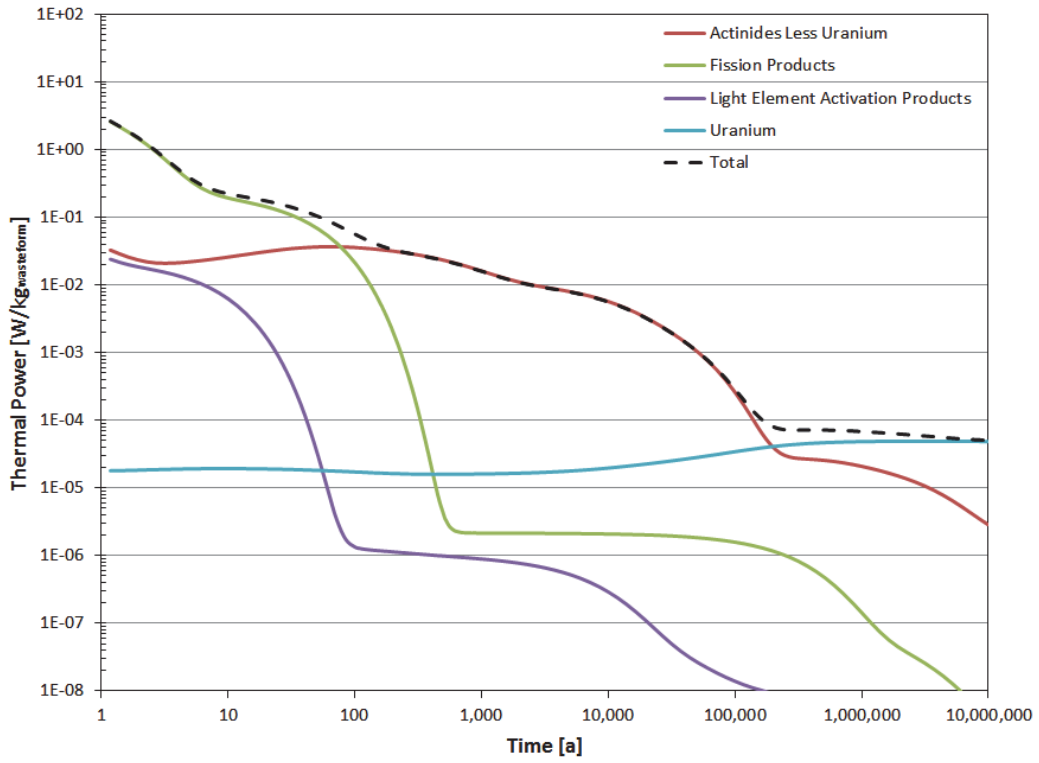


Figure 12: Thermal Power of CANDU Fuel

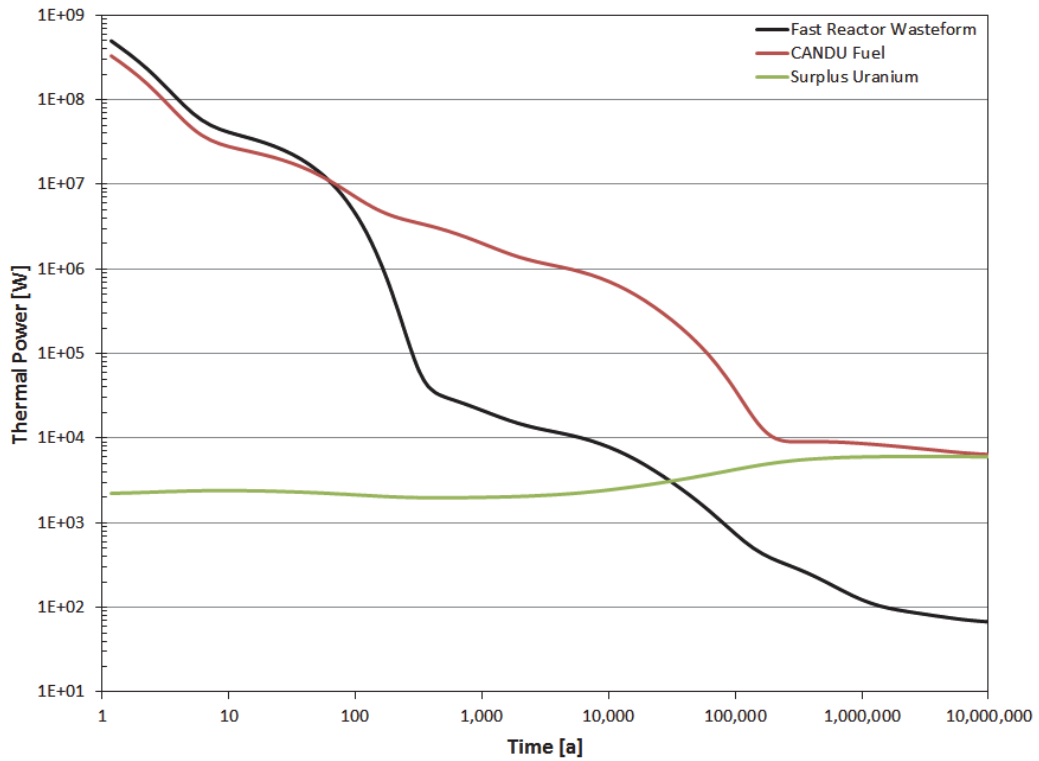


Figure 13: Total Thermal Power for All CANDU Fuel, Fast Reactor Wasteforms and Surplus Uranium

## 4. UNSHIELDED DOSE ASSESSMENT

The purpose of this section of the assessment is to calculate the dose rate to a person standing at varying distances (0.3 m to 10 m) from an unshielded fast reactor wasteform as a function of time in comparison with CANDU used fuel, as another measure of the hazard of this reprocessing wasteform.

The calculations are performed using MicroShield v9.05 (Grove Software Inc., 2012).

### 4.1 MODELLING PARAMETERS

#### 4.1.1 Dimensions

The ceramic waste is assumed to be cylindrical, 55.6 cm long and have a radius of 35 cm (Section 2.3.1).

#### 4.1.2 Composition of Materials

The contents of the fast reactor wasteform are assumed to be a homogeneous mixture of 64% zeolite, 25% borosilicate glass, 8% fission products, uranium, TRUs and light element activation products and 3% waste salt. The density of waste is 1.87 g/cm<sup>3</sup>.

The composition of the zeolite (Table 2), borosilicate glass (Table 3), waste products (Table 4), and waste salts (Table 5) are modelled using the Custom Material Tool in MicroShield. Due to limitations in MicroShield, the large number of fission products, actinides, and waste salts was reduced to a few main constituents. It should be noted that the materials and radionuclides included in Table 2 through Table 5 are strictly for shielding calculations.

**Table 2: Composition of Zeolite (Ugal et al. 2010)**

Component	Weight Percent (%)
Al <sub>2</sub> O <sub>3</sub>	37.3
CaO	0.25
Fe <sub>2</sub> O <sub>3</sub>	1.3
K <sub>2</sub> O	0.48
MgO	0.27
N <sub>2</sub> O	15.1
SiO <sub>2</sub>	42.9
TiO	2.4

**Table 3: Composition of Borosilicate Glass (Corning, 2015)**

Component	Weight Percent (%)
Al <sub>2</sub> O <sub>3</sub>	3
B <sub>2</sub> O <sub>3</sub>	13
Na <sub>2</sub> O	4
SiO <sub>2</sub>	80

**Table 4: Dominant Waste Products (Tait et al. 2000)**

Component	Dominant Elements	Weight Percent (%)
Uranium	U	40.6
Fission Products	Tc, Zr, Nd, Rb, Pd, Sm	59.1
TRU	Pu, Th	0.34

**Table 5: Composition of Waste Salt (Priebe and Bateman, 2006)**

Component	Weight Percent (%)
KCl	42.5
LiCl	42.5
NaCl	15.0

#### 4.1.3 Source Activity

The initial radioactivity for each radionuclide in Appendix A was input into Microshield for the fast reactor wasteform. The activity concentration for later times is calculated in MicroShield using the Decay Tool. The ICRP-107 library (ICRP, 2008) is used for nuclide half-lives and branching ratios.

#### 4.1.4 Buildup Factor

The buildup factor accounts for the photon scattering through shielding materials. This model assumes that the only buildup material is the wasteform, since it is the only shielding material in the path of the photons in this assessment.

#### 4.1.5 Integration Parameters

A 40×40×40 mesh was used in all calculations.

## 4.2 DOSE RESULTS

Figure 14 summarizes the results of the calculations showing the dose rate (in mSv/a) as a function of the age of the waste for various distances from the surface of a 400-kg fast reactor wasteform. Figure 15 shows the dose rate at 10 m (in (mSv/a)/kg) as a function of time for the fast reactor wasteform and for a used CANDU fuel bundle Medri (2012). It should be noted that the dose rates for the CANDU fuel bundle calculated in Medri (2012) assume a high (95<sup>th</sup> percentile) burnup of 280 MWh/kgU. Consequently the dose rate for a more comparable lower burnup bundle would be somewhat lower due to the reduced radionuclide inventory.

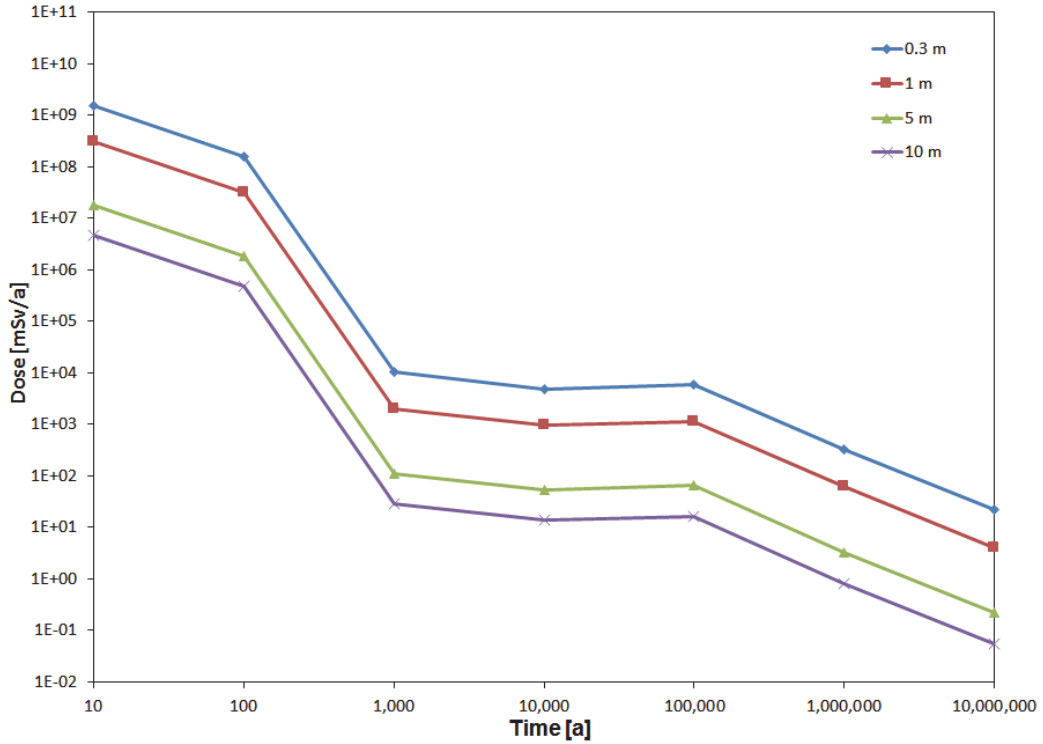


**Figure 14: Dose Rate from the Fast Reactor Wasteform as a Function of Decay Time and Distance**

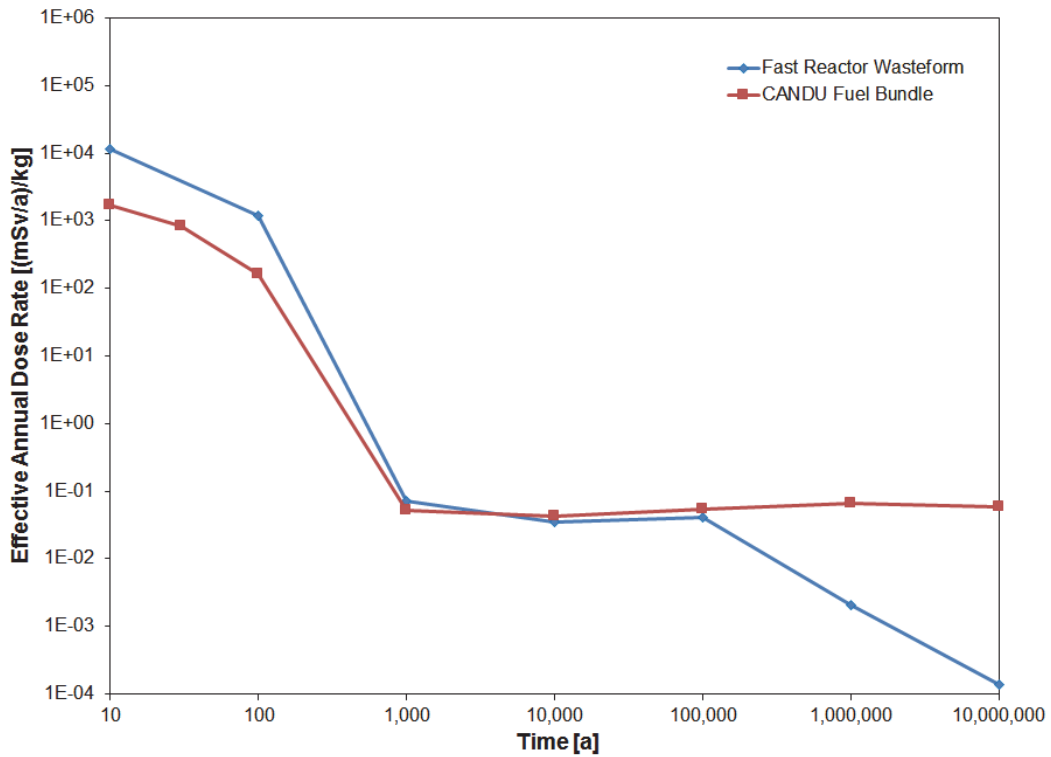


**Figure 15: Annual Dose Rate at 10 m from a Fast Reactor Wasteform and a CANDU Fuel Bundle per Unit Mass**

The dose rates from the fast reactor wasteform, as shown in Figure 14, are dominated by fission products. For the first 1,000 years, the dose is primarily due to Cs-137 and Ba-137m. Between 1,000 years and 1,000,000 years, the dose is primarily due to long lived fission products (Sn-126, Zr-93, Nb-93m, Tc-99, and Pd-107).

Figure 15 shows the annual dose rate on a per kg basis from the fast reactor wasteform are similar to those from the used fuel bundle. Initially the dose rate from the fast reactor wasteform is approximately six times higher than the CANDU fuel; however, after 1,000 years several of the shorter lived fission products have decayed and the fast reactor wasteform dose rate is a factor of 1.5 times lower than the CANDU fuel bundle. Beyond 100,000 years the dose rate for the fast reactor wasteform remains dominated by long lived fission products but starts to decrease as some of the longer lived fission products decay (notably Sn-126). The CANDU fuel dose rate remains relatively flat due to the decay and ingrowth of the uranium daughters (e.g. Bi-210 and Po-210). In the fast reactor wasteform, the relative inventory of uranium is much lower and consequently its daughters only contribute significantly to the dose beyond 10 million years.

## 5. POSTCLOSURE SAFETY

Sections 3 and 4 show that on a per kg of wasteform basis the fast reactor wasteform from reprocessing and the CANDU fuel are broadly similar in terms of radioactivity, radiotoxicity, thermal power and unshielded dose rate. The fast reactor wasteform has a larger initial radioactivity, radiotoxicity and thermal output due to the larger fission products inventory. After several hundred years the fast reactor wasteform is less hazardous than a comparable amount of spent CANDU fuel. However, the fast reactor wasteform would still be quite dangerous and would be considered long-lived high level nuclear waste<sup>2</sup>, would require regulatory control and ultimately need to be managed of in a safe manner.

This section considers the consequences of two options for the long term management of the fast reactor wasteform produced by reprocessing spent CANDU and fast reactor fuel. In the first option, the consequence of placing the fast reactor wasteforms in a deep geological repository similar to that planned for spent CANDU fuel is discussed. In the second option, the consequence of placing the fast reactor wasteforms in a surface landfill site is discussed.

### 5.1 DEEP GEOLOGICAL REPOSITORY

The purpose of a deep geological repository is to safely isolate spent nuclear fuel or nuclear wastes from the surface environment through a number of passive barriers. In the case of spent CANDU fuel, these barriers consist of the used fuel bundle, a steel and copper container, bentonite clay, and hundreds of meters of low permeability rock. It is intended that these barriers will remain intact essentially indefinitely. Postclosure safety assessments (NWMO 2012, NWMO, 2013) show such a facility could meet regulatory requirements for the protection of people and the environment.

<sup>2</sup> IAEA (1994) states “an exact boundary level for High Level Waste (HLW) is difficult to quantify without precise planning data for individual facilities”. However it states, “Typical activity levels are in the range of  $5 \times 10^4$  to  $5 \times 10^5$  TBq/m<sup>3</sup>, corresponding to a heat generation rate of about 2 to 20 kW/m<sup>3</sup> for decay periods of up to about ten years after discharge of spent fuel from a reactor. From this range, the lower value of about 2 kW/m<sup>3</sup> is considered reasonable to distinguish HLW from other radioactive waste classes, based on the levels of decay heat emitted by high level waste such as those from processing spent fuels”. Based on this definition the fast reactor wasteform would be considered high level waste.

The long term radiological impacts of a deep geological repository containing ceramic wastes on people and the environment would require further assessment. However, some general conclusions can be inferred from the results of a repository containing spent CANDU fuel. NWMO (2012, 2013) show that the long-term dose consequences of a repository containing CANDU fuel are primary a result of I-129, a mobile (soluble and non-sorbing), long lived ( $t_{1/2} = 1.57 \times 10^7$ ) fission product. Other significant dose contributors are either fission products or light element activation products and include Cs-135, C-14, Cl-36, Se-79, Ni-59 and Ca-41. Despite uranium and TRUs having long half-lives and making up the bulk of the spent CANDU fuel these species do not contribute significantly to the total dose. This is largely due the durability (i.e. low solubility) of the CANDU fuel and the immobile nature of these species (they are highly insoluble and sorb readily onto a number of minerals in the bentonite and rock).

If a parallel is drawn between a repository containing spent CANDU fuel and one containing fast reactor waste from reprocessing all this CANDU fuel, one would expect higher dose consequences from the fast reactor wastefoms (in a similar container and geological setting) given that it would have a higher fission product inventory. Obviously, the dose consequences would depend on a number of factors including the degradation rate of wasteform. However, it is likely that a deep geological repository could be designed to safely store the glass-ceramic wastefoms from reprocessing.

## **5.2 SURFACE DISPOSAL (LANDFILL) ASSESSMENT**

As shown in earlier sections, the radioactivity and radiotoxicity of the fast reactor wastefoms drops significantly over the first 300 years after discharge. The purpose of this assessment is to evaluate the long term dose consequences assuming the ceramic wastes are placed in a near surface landfill after 300 years.

Essentially, this assessment tests a contention that beyond 300 years the wasteform containing fission products need no longer be considered (long lived) nuclear waste. In reality a number of nuclear regulations would apply to the fast reactor wasteform given the considerable level of radioactivity. However, in this assessment these requirements will be ignored and the near surface disposal evaluated.

Figure 16 shows the conceptual design for a generic double lined landfill as described in MoE (2012). The conceptual landfill model is described in Section 5.2.1 and a detailed description of the model data and assumptions are provided in Section 5.2.2. The model theory and equations are described in Appendix B.

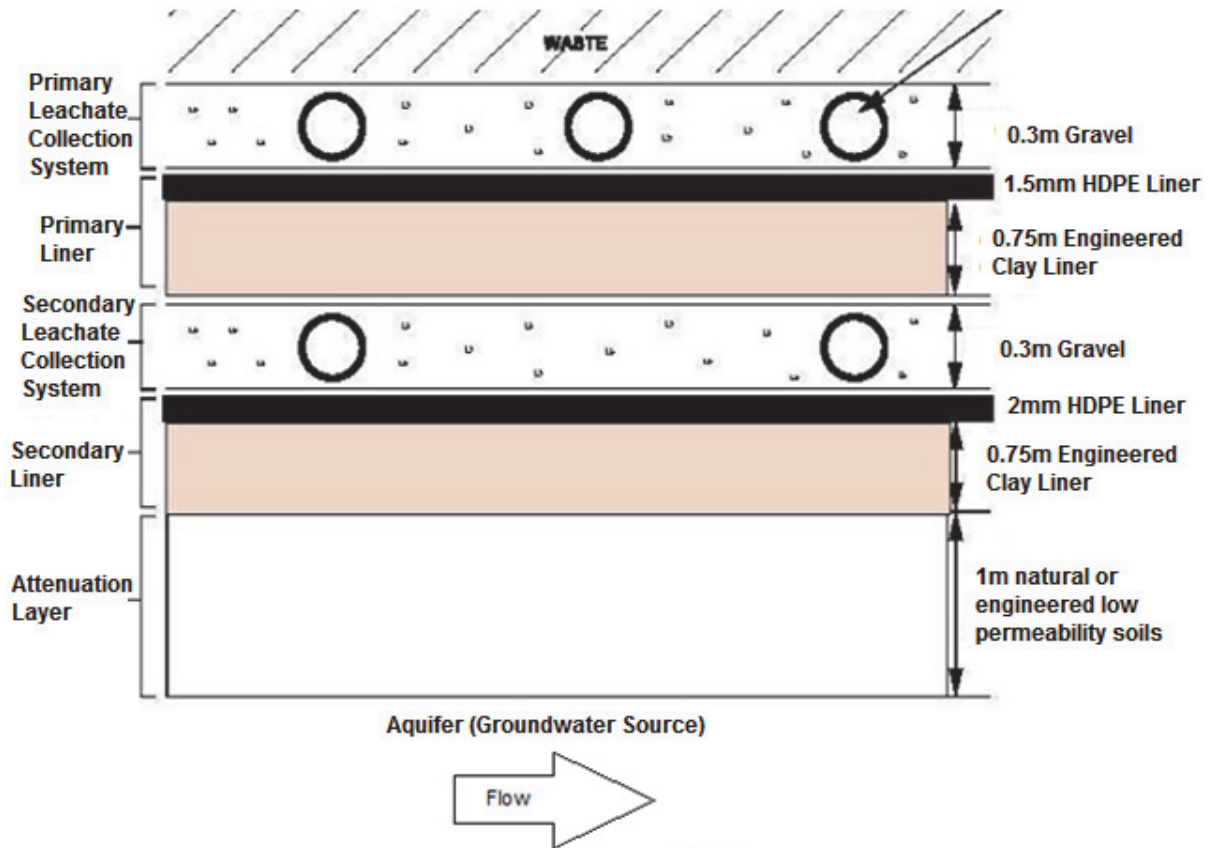


**Figure 16: Generic Design Option II - Double Composite Liner**

### 5.2.1 Conceptual Model

The near surface landfill was assessed using a compartment modelling software AMBER v5.7.1 (Quintessa, 2013). Figure 17 shows the conceptual model of the surface landfill. In the model implemented in AMBER, the gravel, clay, and attenuation layers are each represented by a series of five compartments. Each of these compartments has a forward advective and diffusive transport component and a backward diffusive transport component. The series of five compartments are used to approximate dispersion (see Section B.3).

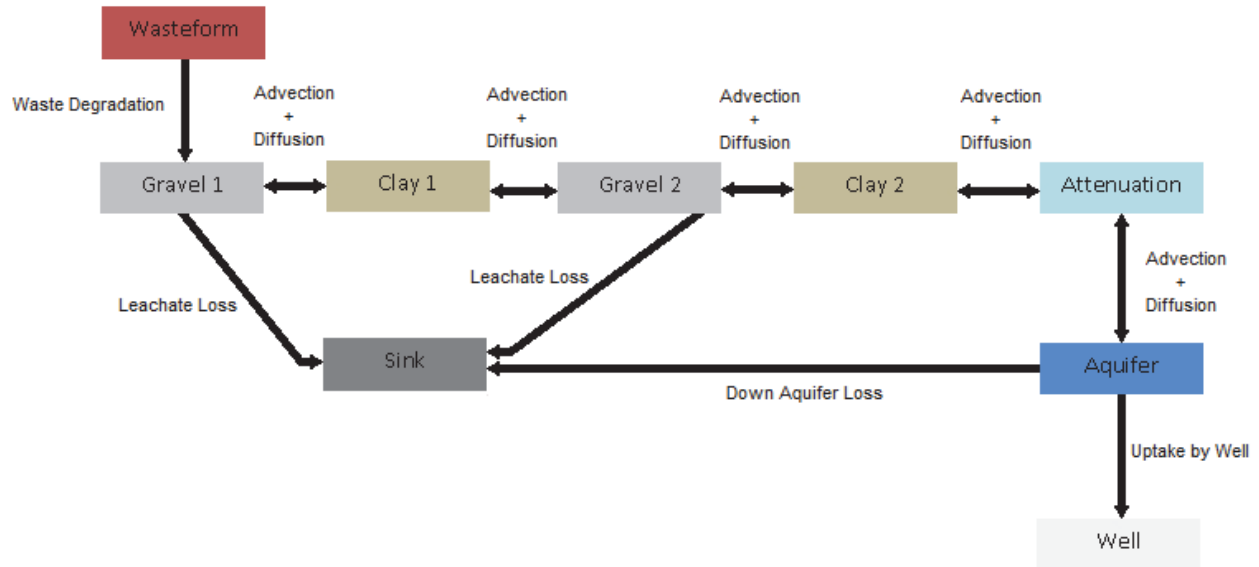


**Figure 17: Conceptual AMBER Model**

After the 300 year cooling period, the wasteform is assumed to be placed in the landfill where it will begin to degrade over time. As the wasteform degrades the radionuclides will migrate through the gravel, liners, clay, attenuation layer and into the aquifer where they will be collected by the well. The primary and secondary leachate collection systems (located in the gravel layers) are assumed to remain intact for 500 and 1000 years respectively after the landfill is built (i.e., the landfill is built and the wastes are emplaced after the 300 year cooling period) (MoE, 2012). It is assumed that 90% of the leachate is collected by the primary and secondary leachate collection systems while they remain intact. For the two stage leachate system, this means that only 1% of the leachate reaches the aquifer for the first 500 years and 10% for the following 500 years. Beyond 1000 years, 100% of the leachate is assumed to migrate into the attenuation layer. As the wasteform degrades, the collected leachate will become radioactive and need to be managed safely. However, for this assessment the leachate will be assumed to be removed from the system and safety managed, and will not be considered further. This model also assumes the clay layers are composed of bentonite clay and remain intact even after the leachate collection systems are no longer active. In addition, the attenuation layer is assumed to have the properties of overburden from Garisto et al. (2012).

The only dose pathway considered in this model is from drinking contaminated water from a well that intercepts the aquifer below the landfill. It is assumed that a well is located 100 m from the landfill site and intercepts the aquifer.

## 5.2.2 Assessment Data

### 5.2.2.1 Radionuclide Inventory and Half-Lives

Section 2.4 describes the basis for the ceramic waste inventory. As described in that section, this analysis assumes 18.9 kg of fission products, 13 kg of uranium, 0.11 kg of TRUs, and 0.0096 kg of light element activation products are present in each 400 kg fast reactor wasteform. The analysis will also assume the composition of the fission products, TRUs, U and light element activation products in the fast reactor wasteform is the same as that of CANDU fuel with a burnup of 220 MWh/kgU. The resulting total inventory for each radionuclide is listed

in Appendix A. The radionuclide half-lives used in this assessment are also listed in Appendix A and are from the ENDF/B-VII.1 dataset (Chadwick et al. 2011).

#### 5.2.2.2 Release Rate from the Fast Reactor Wasteform

Release of radionuclides from the fast reactor wasteform is assumed to occur via leaching and congruent dissolution of the fast reactor wasteform. Release rates from the wasteform depend on a number of factors including: the temperature around the waste packages, groundwater composition, radiation levels, and the elemental composition of the fast reactor wasteform.

Initially, the release of radionuclides from the fast reactor wasteform is due to the leaching. Table 6 lists a variety of normalized release rates (in kg/m<sup>2</sup>/a) measured for glass-zeolite wasteforms. The normalized release rate (NRR) was experimentally measured in Priebe and Bateman (2006), Frank et al. (1997) and Morss et al. (1999). The normalized release rates for a given element, *i*, are determined and by equation (1).

$$NRR_i = \frac{C_i \cdot V}{f_i \cdot A \cdot t} \quad (1)$$

Where,

*C<sub>i</sub>* is the concentration of element *i* in the leachate (kg/L);

*V* is the volume of the leachate (L);

*f<sub>i</sub>* is the mass fraction of the element *i* in the solid;

*A* is the surface area of the sample (m<sup>2</sup>); and

*t* is the duration of the test in years (a).

Table 6 also shows the normalized release rates are somewhat dependent on how the sample was prepared for experimental tests. The finely ground, powdered and wafered samples from Priebe and Bateman (2006), Frank et al. (1997) and Morss et al. (1999) all had higher leaching rates than the crushed samples from Morss et al. (1999) and it is likely that the leaching rate from an intact wasteform would be lower than those listed here. Table 6 also shows that the leaching rates are element dependent and the averaged elemental release rate for each species listed in Table 6 will be assumed for this study. Table 6 does not include leaching rates for all the elements of interest in this study. Consequently, the average leaching rate for all available elements will be assumed for the elements not listed in Table 6.

**Table 6: Normalized Release Rates [kg/m<sup>2</sup>/a]**

Element	Priebe & Bateman (2006) <sup>a</sup>	Frank et al. (1997) <sup>b</sup>	Frank et al. (1997) <sup>c</sup>	Morss et al. (1999) <sup>d</sup>	Morss et al. (1999) <sup>e</sup>	Average
Al	2.4x10 <sup>-4</sup>	4.0x10 <sup>-3</sup>	4.4x10 <sup>-3</sup>	-	-	3.6x10 <sup>-3</sup>
B	7.2x10 <sup>-3</sup>	5.8x10 <sup>-2</sup>	5.1x10 <sup>-3</sup>	-	-	2.4x10 <sup>-2</sup>
Ba	-	<7.3x10 <sup>-4</sup>	<7.3x10 <sup>-4</sup>	-	-	7.3x10 <sup>-4</sup>
Ce	-	2.3x10 <sup>-3</sup>	<1.8x10 <sup>-3</sup>	5.1x10 <sup>-3</sup>	2.4x10 <sup>-5</sup>	2.3x10 <sup>-3</sup>
Cl	1.1x10 <sup>-1</sup>	4.0x10 <sup>-1</sup>	5.8x10 <sup>-3</sup>	-	-	1.7x10 <sup>-1</sup>
Cs	-	2.3x10 <sup>-3</sup>	1.0x10 <sup>-3</sup>	-	-	1.7x10 <sup>-3</sup>
K	1.2x10 <sup>-2</sup>	1.1x10 <sup>-1</sup>	2.1x10 <sup>-3</sup>	-	-	4.1x10 <sup>-2</sup>
La	-	<1.2x10 <sup>-3</sup>	<1.2x10 <sup>-3</sup>	-	-	1.2x10 <sup>-3</sup>
Li	3.1x10 <sup>-2</sup>	2.6x10 <sup>-1</sup>	1.9x10 <sup>-2</sup>	-	-	1.0x10 <sup>-1</sup>
Na	2.0x10 <sup>-2</sup>	2.1x10 <sup>-1</sup>	4.4x10 <sup>-3</sup>	-	-	7.8x10 <sup>-2</sup>
Nd	-	<1.8x10 <sup>-3</sup>	<1.8x10 <sup>-2</sup>	5.1x10 <sup>-3</sup>	2.4x10 <sup>-5</sup>	6.3x10 <sup>-3</sup>
Pr	-	<1.8x10 <sup>-2</sup>	<1.8x10 <sup>-2</sup>	-	-	1.8x10 <sup>-2</sup>
Rb	-	<7.7x10 <sup>-1</sup>	<7.7x10 <sup>-1</sup>	-	-	7.7x10 <sup>-1</sup>
Si	2.5x10 <sup>-3</sup>	1.6x10 <sup>-3</sup>	3.5x10 <sup>-3</sup>	-	-	2.5x10 <sup>-3</sup>
Sm	-	<7.3x10 <sup>-4</sup>	<7.3x10 <sup>-4</sup>	-	-	7.3x10 <sup>-4</sup>
Sr	-	<9.5x10 <sup>-4</sup>	<9.5x10 <sup>-4</sup>	-	-	9.5x10 <sup>-4</sup>
U	-	-	-	5.3x10 <sup>-3</sup>	5.3x10 <sup>-5</sup>	2.7x10 <sup>-3</sup>
Y	-	<1.8x10 <sup>-3</sup>	<1.8x10 <sup>-3</sup>	-	-	1.8x10 <sup>-3</sup>
Overall Average						6.8x10 <sup>-2</sup>

**Notes:**

<sup>a</sup> NRR for ground (75µm diameter) glass bonded sodalite wasteform.

<sup>b</sup> NRR for powdered hot isostatic pressed glass bonded zeolite wasteform.

<sup>c</sup> NRR for powdered hot isostatic pressed glass bonded sodalite wasteform.

<sup>d</sup> Based off 90 day NRR for wafered glass bonded sodalite wasteform.

<sup>e</sup> Based off 90 day NRR for crushed glass bonded sodalite wasteform.

It should be noted that the leaching rates listed in Table 6 are derived from leaching experiments over a relatively short experiment time (7 to 90 days). Even over this short experimental duration the leaching rate was shown to decrease with time as radionuclides near the exposed surface of the samples are removed. Overall, it is unlikely that these leaching rates will persist over time periods considered in this study. Section 5.2.3 examines the effect of varying the time the leaching rate remains active on the dose results.

In reality, the loss of radionuclides from the fast reactor wasteform may be limited by the congruent dissolution of the wasteform itself. However, the dissolution mechanism for glass-zeolite ceramics is not well established (Myers et al. 1997). It is expected that the dissolution reaction will either be surface-controlled, as in the case of glass dissolution, or diffusion-controlled. Diffusion-controlled reaction rates will always be less than or equal to a surface-controlled rate. By contrast, the mechanism by which silicate glasses dissolve is very well studied. There is general agreement by those studying nuclear waste glasses that the mechanism of glass dissolution is one of congruent dissolution, followed by precipitation of mineral phases as the leachate becomes saturated with respect to those phases. It is also generally agreed that the rate-limiting step in the dissolution mechanism involves only silicic acid (H<sub>4</sub>SiO<sub>4</sub>) (Myers et al. 1997).

Myers et al. (1997) estimate the congruent dissolution rates for the silicate glass to be about  $3 \times 10^{-3}$  g/m<sup>2</sup>/day at 70°C and pH 8. Similarly, Pierce et al. (2007) estimates the glass dissolution rate to be  $1.2 \times 10^{-3}$  g/m<sup>2</sup>/day. Given the lack of ceramic dissolution rates this study will assume fast reactor wastefrom will dissolve at the larger rate of  $3 \times 10^{-3}$  g/m<sup>2</sup>/day or  $1.1 \times 10^{-3}$  kg/m<sup>2</sup>/a.

### 5.2.2.3 Solubility Limits

Another factor limiting the release of radionuclides from the fast reactor wastefrom is the solubility of a given species. If an element is insoluble it will precipitate into an immobile solid once it is released from the fast reactor wastefrom. This study will assume elemental solubility limits from Gobien and Garisto (2012) (see Appendix A). In this study all isotopes of a given element contribute to the elemental solubility limit proportional to the isotopic abundance of the species.

### 5.2.2.4 Landfill Transport Properties

In this assessment, the clay layers in the landfill are assumed to be bentonite clay, and the attenuation layer is assumed to be overburden. Data for the clay and the attenuation layers are taken from Garisto et al. (2012) and gravel data are taken from an online engineering materials database [www.EngineeringToolBox.com](http://www.EngineeringToolBox.com). Appendix A lists the nuclide dependent transport parameters (diffusion coefficients and sorption coefficients) used in this assessment (Gobien and Garisto, 2012) and Table 7 lists the layer thicknesses (MoE, 2012), porosities and densities (Garisto et al., 2012).

**Table 7: Landfill Transport Properties**

Parameter	Units	Gravel	Clay	Attenuation
Porosity	-	0.4	0.43	0.42
Density	kg/m <sup>3</sup>	1201	1571	1537
Thickness	m	0.3	0.75	1

The infiltration rate through the landfill is assumed to be 0.15 m/a (MoE, 2012).

### 5.2.2.5 Aquifer and Well Properties

It is assumed that the aquifer transport is advectively dominated. As illustrative values for a hypothetical site, the aquifer properties are taken from Macfarlane et al. (1983) which describes a sand aquifer near a landfill site in Southern Ontario. In that study, the average linear velocity was estimated to range from 8 m/a to 14 m/a, with a porosity of 0.38, density of 1760, and water-table slope of 0.003. This assessment assumes an average linear velocity of 11 m/a meaning the contaminant plume will reach the well shortly after it migrates through the attenuation layer.

MoE (2012) requires a 100 m buffer area around the landfill to provide space in which contaminant attenuation may occur. For this assessment, a drinking water well is assumed to exist at the boundary of the 100 m buffer area. The well is assumed to pump at a rate of 911 m<sup>3</sup>/a as in Garisto et al. (2012), which corresponds to a self-sufficient farming family using the well for irrigation and domestic water. This is consistent with the assumption used in deep geological repository safety assessments (NWMO, 2012). The fraction of contaminants captured by the well must also be considered and is conservatively assumed to be 1. It should be noted that since the only dose pathway considered in this assessment is via drinking contaminated well water the dose results will be directly proportional to the well capture fraction

and could be significantly lower if a less conservative well capture fraction was adopted. That in turn would depend in part on where the well was assumed to be located in the far future.

#### 5.2.2.6 Dose Pathway Data

In this assessment the only dose pathway considered is ingestion of contaminated well water. The water ingestion rate is assumed to be 0.84 m<sup>3</sup>/a which corresponds to the 90<sup>th</sup> percentile value from CSA (2008). The ingestion dose coefficients are from ICRP (1996) and are listed in Appendix A. It should be noted that several short lived daughters have an ingestion dose coefficient of zero because their contribution has been included in the parent radionuclide ingestion dose coefficient.

### 5.2.3 Dose Results

Figure 18 shows the estimated dose rates (in Sv/a) as a function of time if all 78,553 waste packages are disposed of in a single landfill after a 300 year cooling period. Figure 18 also shows the effect of a variety of wastefrom degradation modes on the dose rate. Overall the dose consequences are high and exceed or approach the public dose limit of 1 mSv/a. For the most conservative degradation mode the public dose limit is exceeded by a factor of approximately 1000.

The black curve in Figure 18 is the most conservative degradation mode and assumes that leaching is the only mechanism by which radionuclides are removed from the wastefrom. Furthermore, all elements are assumed to be soluble and do not precipitate. In this mode all the radionuclides are leached from the wastefrom in a few thousand years. The peak dose occurs at 2000 years and is due to fission products and activation products, primarily I-129 and C-14. The rise in dose at later times is due to the higher sorbing and therefore slower moving uranium daughters, specifically, Ra-226.

The blue curve in Figure 18 assumes the leaching phase is not sustainable and only remains active for the first ten years after placement of the wastefrom in the landfill. Radionuclides are then released via congruent dissolution of the fast reactor wastefrom. Note that congruent dissolution also occurs during the leaching phase and all elements are assumed to be soluble. The peak after a few hundred years is due to I-129, Cl-36 and C-14 released in the leaching phase. Between 1000 and 10,000 years the dose is due to the congruent release of I-129 and the peak at later times (>100,000 years) remains due to Ra-226.

The red curve is the least conservative degradation mode and assumes the same ten year leaching phase and congruent dissolution of the wastefrom. However, for this mode a species is assumed to precipitate if its concentration exceeds the element solubility limit. The initial peak is still due to I-129, Cl-36 and C-14 but is slightly lower due to the reduction in the contribution from C-14. The dose at long times is due to the congruent release of I-129 as the dose due to the insoluble actinides and their daughters has been significantly reduced. Sensitivity to other model parameters will be explored using this degradation mode.

Figure 19 examines four sensitivity cases for the least conservative degradation mode from Figure 18 (red curve). The first case examines the effect of extending the leaching phase duration from 10 years to 100 years. The second case studies the effect of increasing the congruent dissolution rate by a factor of 10. The third case looks at the influence of the leachate collection system assumed to be active in the landfill. The final case examines the influence of the well capture fraction on the dose rate.

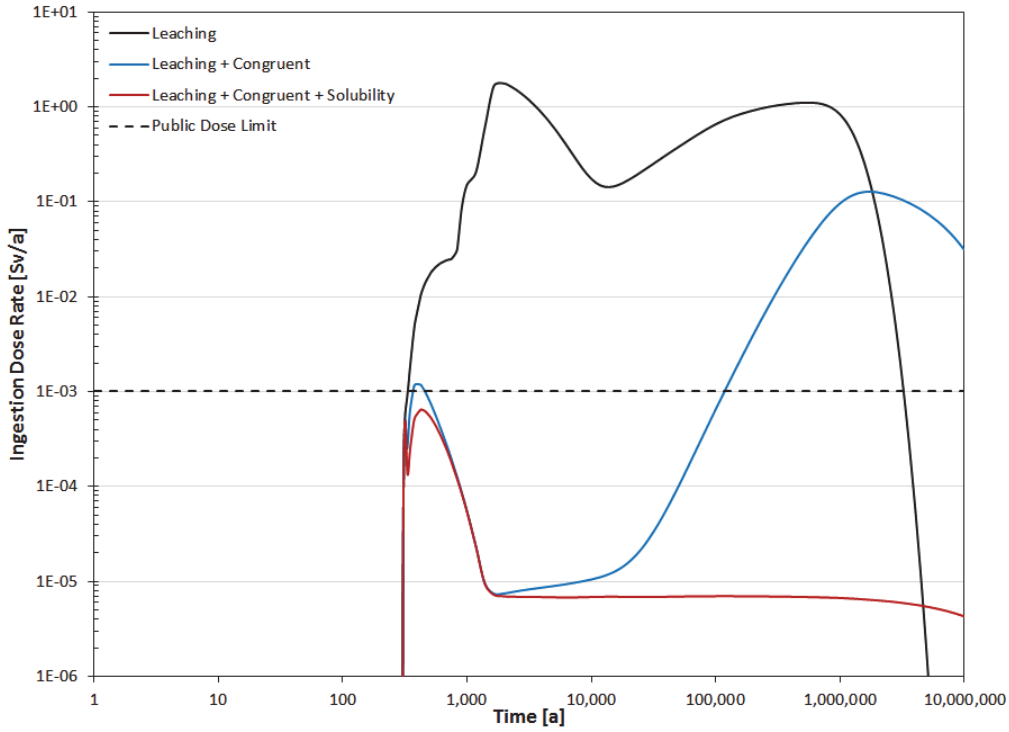


**Figure 18: Effect of Wasteform Degradation Model on Dose Rate as a Function of Time for a Delay of 300a**

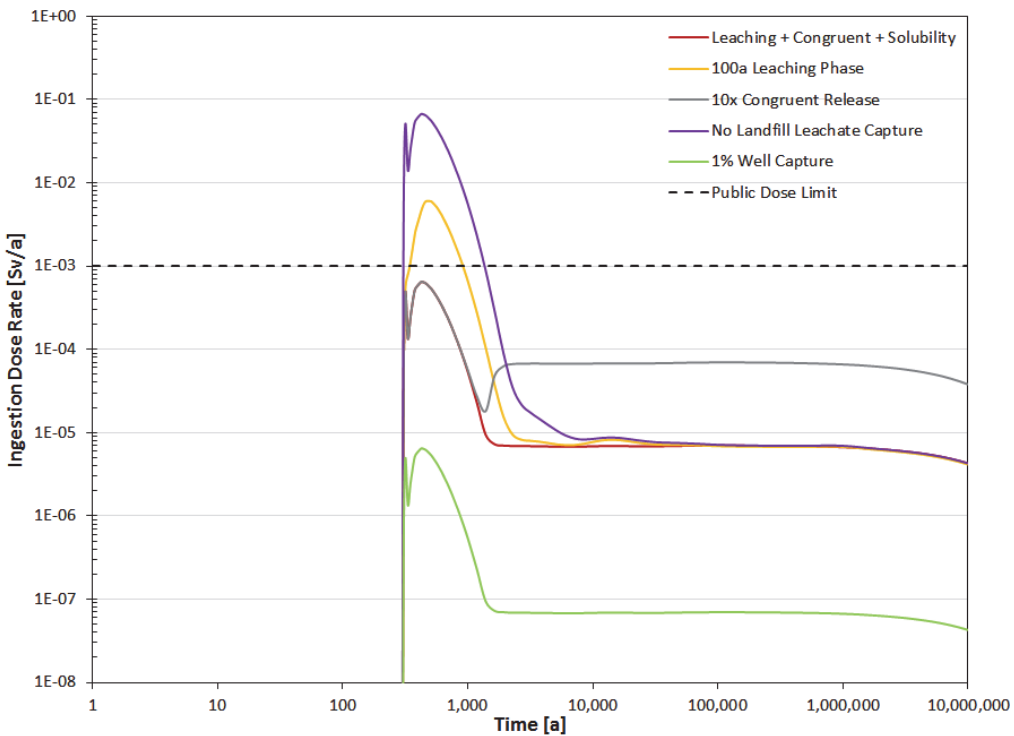


**Figure 19: Effect of Model Assumptions on Dose Rate as a Function of Time**

In the first sensitivity case (yellow line) extending the leaching phase has a significant impact on the dose results. The longer the leaching phase remains active the larger the initial peak becomes. The leaching phase peak dose is due to I-129, Cl-36 and C-14 and the peak dose has increased by a factor of about 9 relative to the base case (red curve). The remainder of the dose curve, which is controlled by the congruent dissolution of the wasteform, remains unchanged.

In the second sensitivity case the congruent dissolution rate is increased by a factor of 10. The initial peak controlled by the leaching phase remains unchanged from the base case but the dose rate curve at later times is a factor of 10 higher.

In the third sensitivity case (purple line) the leachate collection system in the landfill is no longer assumed to be present. This means the 100% of the leachate is able to migrate through the landfill (as opposed to 1% between year 300 and 800 and 10% between years 800 and 1300) and into the aquifer below. The dose curve remains controlled by the same radionuclides (I-129, Cl-36 and C-14). However, by removing the leachate collection system the peak dose is a factor of 100 higher. This suggests that the leachate removed from the system would also pose a significant radiological hazard.

Finally, the fourth sensitivity case (green line) shows that, as expected, the dose rates are proportional to the assumed well capture fraction and decrease by a factor of 100. A more robust model of the aquifer and well could determine an appropriate well capture fraction and for a fast flowing aquifer like the one assumed in this study the well capture fraction could be quite small.

This analysis has not considered disruption of the landfill at long times by human or natural forces.

These results indicate that surface disposal would result in unacceptable dose predictions, or at best has a small margin of safety given the uncertainties at long times, and indicates that that near-surface disposal of the fast reactor wasteforms is not appropriate.

## **6. SUMMARY**

This report estimates the hazard associated with waste produced by reprocessing spent CANDU fuel and burning this in fast reactors. The results of this work indicate that the glass-ceramic fast reactor wasteform could have a level of radioactivity, radiotoxicity, thermal power and unshielded dose rate broadly similar to that of a CANDU fuel bundle on a per kg of wasteform basis. The fast reactor wasteform is more hazardous in the short term, and the spent CANDU fuel is more hazardous in the long term.

Table 8 presents a quantitative comparison based on the total amount of waste. The reprocessed / fast reactor wastes correspond to a scenario that generates a further total amount of energy that is roughly comparable to that from the initial spent CANDU fuel.

A simplified postclosure assessment assuming disposal of the fast reactor wasteform after a 300 year cooling period in a modern surface landfill shows that the doses to a person drinking water from a well that intercepts an aquifer near the landfill could be much higher than public dose limits. The dose consequences in this hypothetical scenario are controlled by the fission products and activation products in the wasteform, specifically I-129, Cl-36 and C-14. At long times daughters of U-238 can dominate the dose if solubility limits are not considered.

Sensitivity cases show that the simple model used to estimate dose consequences is sensitive to some parameters but overall the dose consequences from disposal of reprocessing waste in a near surface facility are expected to be high even without considering the additional processes that would affect this facility in the long term.

This analysis has made several simplifying assumptions as described in the report. However, it is unlikely that wastes from the reprocessing of CANDU and fast reactor fuel would be considered anything other than high level waste. Such wastes are comparable to CANDU fuel in many ways, would remain hazardous for very long times, would need to be carefully managed and would ultimately need to be disposed of in a safe manner similar to the existing inventories of spent CANDU fuel.

**Table 8: Summary of the Long-Term Characteristics of the Total CANDU and Fast Reactor Wastes**

Parameter	Used CANDU Fuel	Waste from Reprocessed CANDU and Fast Reactors*
Waste Mass [Mg]	101,000 (used fuel bundles)	31,400 (ceramic-glass wasteform)
Total Radioactivity [Bq]		
At 10 yrs	$3.95 \times 10^{20}$	$5.60 \times 10^{20}$
At 300 yrs	$4.40 \times 10^{18}$	$6.35 \times 10^{17}$
At 100,000 yrs	$6.17 \times 10^{16}$	$2.63 \times 10^{16}$
Total Radiotoxicity [Sv]		
At 10 yrs	$4.13 \times 10^{12}$	$5.32 \times 10^{12}$
At 300 yrs	$8.91 \times 10^{11}$	$1.45 \times 10^{10}$
At 100,000 yrs	$1.12 \times 10^{10}$	$1.40 \times 10^8$
Total Thermal Power [W]		
At 10 yrs	$2.7 \times 10^7$	$4.13 \times 10^7$
At 300 yrs	$3.6 \times 10^6$	$7.70 \times 10^4$
At 100,000 yrs	$3.7 \times 10^4$	$7.43 \times 10^2$

\*Not including 99,000 Mg depleted uranium, nor residual fuel in fast reactor cores.

**REFERENCES**

- ANL (Argonne National Laboratory). 2012. Pyroprocessing Technologies: Recycling Used Nuclear Fuel for a Sustainable Energy Future. Argonne National Laboratory Brochure. Argonne, IL, USA.
- Berger, J. and R. Benedict. 2011. An Integrated Mass Balance Model for Pyrochemical Processing. *Nuclear Technology* 175, 450-459.
- Cacuci, D.G. (Ed). 2010. Handbook of Nuclear Engineering, Vol. 1 - Nuclear Engineering Fundamentals. Springer Inc. USA.
- Chadwick, M.B., M. Herman, P. Obložinský, M.E. Dunn, Y. Danon, A.C. Kahler, D.L. Smith, B. Pritychenko, G. Arbanas, R. Arcilla, R. Brewer, D.A. Brown, R. Capote, A.D. Carlson, Y.S. Cho, H. Derrien, K. Guber, G.M. Hale, S. Hoblit, S. Holloway, T.D. Johnson, T. Kawano, B.C. Kiedrowski, H. Kim, S. Kunieda, N.M. Larson, L. Leal, J.P. Lestone, R.C. Little, E.A. McCutchan, R.E. MacFarlane, M. MacInnes, C.M. Mattoon, R.D. McKnight, S.F. Mughabghab, G.P.A. Nobre, G. Palmiotti, A. Palumbo, M.T. Pigni, V.G. Pronyaev, R.O. Sayer, A.A. Sonzogni, N.C. Summers, P. Talou, I.J. Thompson, A. Trkov, R.L. Vogt, S.C. van der Marck, A. Wallner, M.C. White, D. Wiarda, P.G. Young. 2011. ENDF/B-VII.1 Nuclear Data for Science and Technology: Cross section, covariances, fission product yields, and decay data. *Nuclear Data Sheets*: 112-12, 2887-2996 (2011).
- Corning. 2015. Properties of Pyrex, Pyrexplus and Low Actinic Pyrex Code 7740 Glasses. Corning, NY, USA.
- CSA (Canadian Standards Association). 2008. Guidelines for calculating derived release limits for radioactive materials in airborne and liquid effluents for normal operation of nuclear facilities. Canadian Standards Association Report CSA-N288.1-08. Toronto, Canada.
- Frank, S.M., K.J. Bateman, T. DiSanto, S.G. Johnson, T.L. Moschetti, M.H. Noy, and T.P. O'Holleran. 1997. Characterization of Composite Ceramic High Level Waste Forms. Materials Research Society Fall 1997 Meeting. December 1-5, 1997. Boston, Massachusetts.
- Garamszeghy, M. 2014. Nuclear Fuel Waste Projections in Canada – 2014 Update. NWMO TR-2014-16. Toronto, Canada.
- Garisto, F., M. Gobien, E. Kremer and C. Medri. 2012. Fourth Case Study: Reference Data and Codes. Nuclear Waste Management Organization Technical Report NWMO TR-2012-08. Toronto, Canada.
- Gobien M. and F. Garisto. 2012. Data for Radionuclide and Chemical Element Screening. Nuclear Waste Management Organization Technical Report NWMO TR-2012-11. Toronto, Canada.
- Grove Software, Inc. 2012. MicroShield v9.05.

- Herrmann, S.D., S.X. Li, M.F. Simpson, and S. Phongikaroon. 2006. Electrolytic Reduction of Spent Nuclear Oxide Fuel as Part of an Integral Process to Separate and Recover Actinides from Fission Products. *Separation Science and Technology*, vol 41, n.10, 1965-1983. 2006.
- IAEA (International Atomic Energy Agency). 1994. Classification of Radioactive Waste – A Safety Guide. Safety Series No. 111-G-1.1. Vienna, Austria.
- ICRP (International Commission on Radiological Protection). 2008. Nuclear decay data for dosimetric calculations. *Annals of the ICRP* 38 (3), ICRP Publication 107. Pergamon Press, Oxford.
- ICRP (International Commission on Radiological Protection). 1996. Age-dependent doses to member of the public from intake of radionuclides: Part 5. Compilation of ingestion and inhalation dose coefficients. *Annals of the ICRP* 26 (1), ICRP Publication 72. Pergamon Press, Oxford.
- Ion, M. 2015. Some Implications of Recycling CANDU Used Fuel in Fast Reactors. Nuclear Waste Management Organization Technical Report NWMO-TR-2015-11. Toronto, Canada.
- Karell, E.J., K.V. Gourishankar, J.L. Smith, L.S. Chow, and L. Redey. 2001. Separation of Actinides from LWR Fuel Using Molten-Salt-Based Electrochemical Processes. *Nuclear Technology*, vol. 136, December 2001. 342-353.
- Kim, J.G., J.H. Lee, I.T. Kim, and E.H. Kim. 2007. Fabrication of a Glass-Bonded Zeolite Waste Form for Waste LiCl Salt. *J. Ind. Eng. Chem.*, Vol 13, No. 2, (2007), 292-298.
- Lee, Y.-K. and M.-H. Kim. 2015. Performance Evaluation of a Transmutation Sodium-Cooled Fast Reactor in Recycling Scenarios. Actinide and Fission Product Partitioning and Transmutation, Proc. Thirteenth Information Exchange Meeting, NEA/NSC/R(2015)2. Seoul, Republic of Korea.
- Li, S.X., and M.F. Simpson. 2005. "Anodic Process of Electrorefining Spent Nuclear Fuel in Molten LiCl-KCl-UCl<sub>3</sub>/Cd System:" *Journal of Mineral and Metallurgical Processing*, Vol. 22, No. 4, November 2005.
- MacFarlane, D.S., J.A. Cheery, R.W. Gillham and E.A. Sudicky. 1983. Migration of Contaminants in Groundwater at a Landfill: A Case Study. *Journal of Hydrology*, Vol 63(1983) pg 1-29. Amsterdam, Netherlands.
- Medri, C. 2012. Used Fuel Bundle Gamma Doses as a function of Distance and Decay Time. Nuclear Waste Management Organization Technical Memorandum APM-TM-03610-29614. Toronto, Canada.
- MoE (Ontario Ministry of the Environment and Climate Change). 2012 Revision. Landfill Standards: A Guideline on the Regulatory and Approval Requirements for New or Expanding Landfilling Sites. Ontario Ministry of the Environment Standard PIBS 7792e.

- Morss, L.R., M.A. Lewis, K. Richmann, and D. Lexa. 1999. Cerium Uranium, and Plutonium Behavior in Glass-Bonded Sodalite, a Ceramic Nuclear Waste Form. Proceedings of the 22<sup>nd</sup> Rare Earth Research Conference. July 11-15, 1999. Argonne, Illinois.
- Myers, B.R., W. Brummond, G. Armantrout, H. Shaw, C.M. Jantzen, A. Jostsons, M. Mckibben, D. Strachan, and J.D. Vienna. 1997. Fissile Materials Disposition Program Technical Evaluation Panel Summary Report: Ceramic and Glass Immobilization Options. UCRL-ID-129315. Livermore, CA, USA.
- Nagarajan, N., B. Prabhakara Reddy, S. Ghosh, G. Ravisankar, K.S. Mohandas, U. Kamachi Mudali, K.V.G. Kuttu, K.V. Kasi Viswanathan, C. Anand Babu, P. Kalyanasundaram, P.R. Vasudeva and B. Raj. 2010. Development of Pyrochemical Reprocessing for Spent Metal Fuels. Energy Procedia, Vol 7 (2011), pg 431-436.
- Nuclear Fuel Cycle Options Catalog. 2014.  
[https://inlportal.inl.gov/portal/server.pt/community/nuclear\\_science\\_and\\_technology/337/online\\_nuclear\\_fuel\\_cycle\\_options\\_catalog](https://inlportal.inl.gov/portal/server.pt/community/nuclear_science_and_technology/337/online_nuclear_fuel_cycle_options_catalog) (accessed July 15, 2015).
- NWMO (Nuclear Waste Management Organization). 2013. Adaptive Phased Management: Postclosure Safety Assessment of a Used Fuel Repository in Sedimentary Rock. Nuclear Waste Management Organization NWMO TR-2013-07. Toronto, Canada.
- NWMO (Nuclear Waste Management Organization). 2012. Adaptive Phased Management: Used Fuel Repository Conceptual Design and Postclosure Safety Assessment in Crystalline Rock. Nuclear Waste Management Organization NWMO TR-2012-16. Toronto, Canada.
- OECD (Organization for Economic Co-operation and Development). 2012. Spent Nuclear Fuel Reprocessing Flowsheet. A Report by the WPFC Expert Group on Chemical Partitioning of the NEA Nuclear Science Committee. NEA/NSC/WPFC/DOC(2012)15. Paris, France.
- Pereira, C., and B.D. Babcock. 1996. Fission Product Removal from Molten Salt Using Zeolite. Second International Symposium on Extraction and Processing for the Treatment and Minimization of Wastes. Scottsdale, Arizona. October 27-30, 1996.
- Phongikaroon, S. 2014. National Analytical Management Program (NAMP) Radiochemistry Webinars – Nuclear Fuel Cycle Series: Introduction to Pyro Processing Technology for Used Nuclear Fuel. U.S. Department of Energy. Carlsbad, New Mexico, USA.
- Pierce, E.M., B.P. Mcgrail, P.F. Martin, J. Marra, B.W. Arey, and K.N. Geiszler. 2007. Accelerated Weathering of High Level and Plutonium-bearing Lanthanide Borosilicate Waste Glasses under Hydraulically Unsaturated Conditions. Journal of Applied Geochemistry, Vol 22(2007) pg 1841-1859.
- Priebe, S., and K. Bateman. 2006. The ceramic Waste Form Process at the Idaho National Laboratory. International Pyroprocessing Research Conference INL/CON-06-11606. Idaho Falls, Idaho.
- Quintessa. 2013. AMBER 5.7 Reference Guide. Quintessa Report QE-AMBER-1, Version 5.7. Henley-on-Thames, United Kingdom.

- Simpson, M.F. 2012. Developments of Spent Nuclear Fuel Pyroprocessing Technology at Idaho National Laboratory. International Pyroprocessing Research Conference INL/EXT-12-25124. Idaho Falls, Idaho.
- SKB (Svensk Kärnbränslehantering AB). 2010. Data report for the safety assessment SR-Site. SKB Technical Report SKB TR-10-52. Stockholm, Sweden
- Tait, J.C., H. Roman and C.A. Morrison. 2000. Characteristics and Radionuclide Inventories of Used Fuel from OPG Nuclear Generating Stations. Volume 1 – Main Report and Volume 2 – Radionuclide Inventory Data. Ontario Power Generation Report 06819-REP-01200-10029-R00. Toronto, Canada.
- Ugal, J.R., H. Karim and A.H. Inam. 2010. Preparation of Type 4A Zeolite from Iraqi Kaolin Characterization and Properties Measurements. Journal of the Association of Arab Universities for Basic and Applied Sciences, Vol. 9, p1-8.
- Williamson, M.A. and J.L. Willit. 2011. Pyroprocessing Flowsheets for Recycling Used Nuclear Fuel. Nuclear Engineering and Technology, 43(4), 329-334.
- Yoo, J.H., C.S. Seo, E.H. Kim, and H.S. Lee. 2008. A Conceptual Study of Pyroprocessing for Recovering Actinides from Spent Oxide Fuels. Nuclear Engineering and Technology, Vol 40, No. 7, p.581-592.

## APPENDIX A – WASTE PROFILES FOR SPENT CANDU FUEL

Appendix A presents the radionuclide specific data used in this assessment.

**Table A-1: Radionuclide Dependent Data Used in the Landfill Assessment**

Radionuclide	Inventory <sup>1</sup> [kg]	Half Life <sup>2</sup> [a]	Effective Diffusion Coefficient [m <sup>2</sup> /a]			Sorption Coefficient [m <sup>3</sup> /kg]			Solubility <sup>9</sup> [mol/m <sup>3</sup> ]	Dose Coefficient <sup>10</sup> [Sv/Bq]
			Gravel <sup>3</sup>	Clay <sup>4</sup>	Attenuation <sup>5</sup>	Gravel <sup>6</sup>	Clay <sup>7</sup>	Attenuation <sup>8</sup>		
Ac-225	1.093E-15	2.74E-02	1.26E-02	4.40E-03	1.32E-02	0	61	2.025	2000	2.43E-08
Ac-227	1.417E-12	2.18E+01								1.10E-06
Ag-108	2.753E-10	4.53E-06	2.14E-02	4.40E-03	2.25E-02	0	0	0.159	0.11	0.00E+00
Ag-108m	3.952E-06	4.38E+02								2.30E-09
Ag-110	2.799E-08	7.80E-06								0.00E+00
Ag-110m	3.152E-04	6.84E-01								2.80E-09
Am-241	4.861E-05	4.33E+02	1.26E-02	4.40E-03	1.32E-02	0	61	7.79	0.223	2.00E-07
Am-242	1.765E-07	1.83E-03								0.00E+00
Am-242m	6.599E-07	1.41E+02								1.90E-07
Am-243	7.381E-05	7.37E+03								2.00E-07
Ar-39	7.449E-06	2.69E+02	1.26E-02	4.40E-03	1.32E-02	0	0	0	2000	0.00E+00
Ar-42	1.292E-13	3.29E+01								4.30E-10
Ba-133	1.517E-06	1.05E+01	1.26E-02	4.40E-03	1.32E-02	0	0.0045	0.4419	0.0026	1.50E-09
Ba-137m	9.502E-08	4.86E-06								0.00E+00
Be-10	1.009E-06	1.51E+06	1.26E-02	4.40E-03	1.32E-02	0	0.0045	1.1	2000	1.10E-09
Bi-208	3.604E-08	3.68E+05	1.26E-02	4.40E-03	1.32E-02	0	35	0.52	0.117	1.16E-09
Bi-210	2.881E-19	1.37E-02								1.30E-09
Bi-210m	5.581E-07	3.04E+06								1.50E-08
Bi-211	2.145E-19	4.06E-06								0.00E+00
Bk-249	3.476E-15	8.76E-01	1.26E-02	4.40E-03	1.32E-02	0	61	4.243	2000	9.70E-10
C-14	6.753E-04	5.70E+03	1.51E-02	4.40E-03	1.59E-02	0	0	0.0052	8.29	5.80E-10

Radionuclide	Inventory <sup>1</sup> [kg]	Half Life <sup>2</sup> [a]	Effective Diffusion Coefficient [m <sup>2</sup> /a]			Sorption Coefficient [m <sup>3</sup> /kg]			Solubility <sup>9</sup> [mol/m <sup>3</sup> ]	Dose Coefficient <sup>10</sup> [Sv/Bq]
			Gravel <sup>3</sup>	Clay <sup>4</sup>	Attenuation <sup>5</sup>	Gravel <sup>6</sup>	Clay <sup>7</sup>	Attenuation <sup>8</sup>		
Ca-41	2.585E-04	1.02E+05	1.26E-02	4.40E-03	1.32E-02	0	0.0045	0.0415	2000	1.90E-10
Ca-45	6.572E-06	4.45E-01								7.10E-10
Cd-109	3.435E-08	1.26E+00	9.08E-03	4.40E-03	9.54E-03	0	0.0045	0.408	0.76	2.00E-09
Cd-113	6.108E-05	8.04E+15								2.50E-08
Cd-113m	7.306E-05	1.41E+01								2.30E-08
Ce-139	3.172E-08	3.77E-01	1.26E-02	4.40E-03	1.32E-02	0	8	15.669	1	2.60E-10
Ce-144	2.800E-01	7.80E-01								5.25E-09
Cf-249	1.810E-16	3.51E+02	1.26E-02	4.40E-03	1.32E-02	0	61	4.243	2000	3.50E-07
Cf-250	7.031E-16	1.31E+01								1.60E-07
Cf-251	1.947E-16	8.98E+02								3.60E-07
Cf-252	1.076E-16	2.64E+00								9.00E-08
Cf-254	3.096E-22	1.66E-01								4.00E-07
Cl-36	1.083E-03	3.01E+05	2.52E-02	4.40E-03	2.65E-02	0	0	0.0001	2000	9.30E-10
Cm-242	1.206E-05	4.46E-01	1.26E-02	4.40E-03	1.32E-02	0	61	7.78	0.223	1.20E-08
Cm-243	1.600E-07	2.91E+01								1.50E-07
Cm-244	6.574E-06	1.81E+01								1.20E-07
Cm-245	4.524E-08	8.50E+03								2.10E-07
Cm-246	6.117E-09	4.76E+03								2.10E-07
Cm-247	2.716E-11	1.56E+07								1.90E-07
Cm-248	8.542E-13	3.48E+05								7.70E-07
Cm-250	5.113E-21	8.30E+03								4.40E-06
Co-58	1.583E-06	1.94E-01	8.83E-03	4.40E-03	9.27E-03	0	0.0045	0.644	1	7.40E-10
Co-60	3.030E-03	5.27E+00								3.40E-09
Cs-134	2.554E-02	2.07E+00	2.65E-02	4.40E-03	2.78E-02	0	0.093	2.167	2000	1.90E-08
Cs-135	6.261E-02	2.30E+06								2.00E-09
Cs-137	6.096E-01	3.01E+01								1.30E-08
Dy-159	1.119E-08	3.95E-01	1.26E-02	4.40E-03	1.32E-02	0	8	1.07	1	1.00E-10

Radionuclide	Inventory <sup>1</sup> [kg]	Half Life <sup>2</sup> [a]	Effective Diffusion Coefficient [m <sup>2</sup> /a]			Sorption Coefficient [m <sup>3</sup> /kg]			Solubility <sup>9</sup>	Dose Coefficient <sup>10</sup>
			Gravel <sup>3</sup>	Clay <sup>4</sup>	Attenuation <sup>5</sup>	Gravel <sup>6</sup>	Clay <sup>7</sup>	Attenuation <sup>8</sup>	[mol/m <sup>3</sup> ]	[Sv/Bq]
Es-254	5.681E-21	7.55E-01	1.26E-02	4.40E-03	1.32E-02	0	61	4.243	2000	2.81E-08
Eu-149	5.944E-14	2.55E-01	1.26E-02	4.40E-03	1.32E-02	0	8	0.553	1	1.00E-10
Eu-150	3.643E-12	3.69E+01								1.30E-09
Eu-152	9.449E-07	1.35E+01								1.40E-09
Eu-154	4.861E-03	8.60E+00								2.00E-09
Eu-155	2.412E-03	4.75E+00								3.20E-10
Fe-55	1.300E-04	2.74E+00	1.26E-02	4.40E-03	1.32E-02	0	0.0045	0.296	2000	3.30E-10
Gd-152	6.486E-06	1.08E+14	1.26E-02	4.40E-03	1.32E-02	0	8	0.4455	1	4.10E-08
Gd-153	1.364E-05	6.58E-01								2.70E-10
H-3	2.209E-03	1.23E+01	1.26E-02	4.40E-03	1.32E-02	0	0	0	2000	1.80E-11
Hf-175	1.215E-06	1.92E-01	1.26E-02	4.40E-03	1.32E-02	0	4	2.025	2000	4.10E-10
Hf-182	1.007E-06	8.90E+06								3.00E-09
Ho-163	4.462E-08	4.57E+03	1.26E-02	4.40E-03	1.32E-02	0	8	1.095	0.067	1.20E-06
Ho-166m	2.409E-06	1.20E+03								2.00E-09
I-129	9.729E-02	1.57E+07	2.52E-02	4.40E-03	2.65E-02	0	0	0.0128	2000	1.10E-07
In-115	2.021E-03	4.41E+14	1.26E-02	4.40E-03	1.32E-02	0	0	0.398	2000	3.20E-08
Ir-192	1.088E-05	2.02E-01	1.26E-02	4.40E-03	1.32E-02	0	0	0.409	2000	1.40E-09
Ir-192m	8.458E-08	2.41E+02								3.10E-10
Ir-194	4.524E-07	2.20E-03								0.00E+00
Ir-194m	4.768E-06	4.68E-01								2.10E-09
K-40	2.914E-04	1.25E+09	1.26E-02	4.40E-03	1.32E-02	0	0.093	0.065	2000	6.20E-09
Kr-81	2.482E-06	2.29E+05	1.26E-02	4.40E-03	1.32E-02	0	0	0	2000	0.00E+00
Kr-85	1.761E-02	1.08E+01								0.00E+00
La-137	5.179E-07	6.00E+04	1.26E-02	4.40E-03	1.32E-02	0	8	0.749	1	8.10E-11
La-138	8.452E-06	1.02E+11								1.10E-09
Lu-176	5.454E-07	3.76E+10	1.26E-02	4.40E-03	1.32E-02	0	8	1.07	2000	1.80E-09
Lu-177	1.875E-07	1.82E-02								5.30E-10

Radionuclide	Inventory <sup>1</sup> [kg]	Half Life <sup>2</sup> [a]	Effective Diffusion Coefficient [m <sup>2</sup> /a]			Sorption Coefficient [m <sup>3</sup> /kg]			Solubility <sup>9</sup> [mol/m <sup>3</sup> ]	Dose Coefficient <sup>10</sup> [Sv/Bq]
			Gravel <sup>3</sup>	Clay <sup>4</sup>	Attenuation <sup>5</sup>	Gravel <sup>6</sup>	Clay <sup>7</sup>	Attenuation <sup>8</sup>		
Lu-177m	1.474E-08	4.39E-01								1.70E-09
Mn-54	2.287E-06	8.54E-01	1.26E-02	4.40E-03	1.32E-02	0	0.0045	0.2749	2000	7.10E-10
Mo-93	3.306E-07	4.00E+03	1.26E-02	4.40E-03	1.32E-02	0	0.089	0.089	0.003	3.10E-09
Na-22	2.216E-12	2.60E+00	1.64E-02	4.40E-03	1.72E-02	0	0.0045	0.2151	2000	3.20E-09
Nb-91	1.817E-11	6.80E+02	1.26E-02	4.40E-03	1.32E-02	0	3	0.756	0.13	1.20E-06
Nb-92	4.795E-08	3.47E+07								1.20E-06
Nb-93m	9.682E-07	1.61E+01								1.20E-10
Nb-94	5.358E-05	2.03E+04								1.70E-09
Nb-95	6.508E-02	9.58E-02								5.80E-10
Nb-95m	7.466E-05	9.88E-03								5.60E-10
Nd-144	2.995E-01	2.29E+15	1.26E-02	4.40E-03	1.32E-02	0	8	1.07	1	1.20E-06
Ni-59	7.073E-04	7.60E+04	8.58E-03	4.40E-03	9.01E-03	0	0.3	0.569	29	6.30E-11
Ni-63	1.261E-04	1.01E+02								1.50E-10
Np-235	3.703E-12	1.08E+00	1.26E-02	4.40E-03	1.32E-02	0	63	0.01755	1.08E-05	2.41E-10
Np-236	1.065E-10	1.53E+05								1.70E-08
Np-237	4.363E-04	2.14E+06								1.10E-07
Np-238	1.804E-06	5.80E-03								9.10E-10
Np-239	1.047E-03	6.45E-03								8.00E-10
Os-185	1.028E-08	2.56E-01	1.26E-02	4.40E-03	1.32E-02	0	0	0.851	2000	5.10E-10
Os-194	2.032E-08	6.00E+00								3.70E-09
P-32	5.798E-06	3.90E-02	1.26E-02	4.40E-03	1.32E-02	0	0	0.0412	2000	2.40E-09
Pa-231	1.179E-07	3.28E+04	1.26E-02	4.40E-03	1.32E-02	0	3	2.304	2.22E-05	7.10E-07
Pa-233	1.903E-05	7.39E-02								8.70E-10
Pb-205	1.416E-06	1.73E+07	1.26E-02	4.40E-03	1.32E-02	0	74	3.612	0.0796	2.80E-10
Pb-210	4.956E-16	2.22E+01								6.90E-07
Pd-107	1.634E-01	6.50E+06	1.26E-02	4.40E-03	1.32E-02	0	5	0.2305	0.0411	3.70E-11
Pm-145	9.587E-09	1.77E+01	1.26E-02	4.40E-03	1.32E-02	0	8	0.5552	1	1.10E-10

Radionuclide	Inventory <sup>1</sup> [kg]	Half Life <sup>2</sup> [a]	Effective Diffusion Coefficient [m <sup>2</sup> /a]			Sorption Coefficient [m <sup>3</sup> /kg]			Solubility <sup>9</sup> [mol/m <sup>3</sup> ]	Dose Coefficient <sup>10</sup> [Sv/Bq]
			Gravel <sup>3</sup>	Clay <sup>4</sup>	Attenuation <sup>5</sup>	Gravel <sup>6</sup>	Clay <sup>7</sup>	Attenuation <sup>8</sup>		
Pm-146	6.931E-07	5.53E+00								9.00E-10
Pm-147	1.285E-01	2.62E+00								2.60E-10
Po-210	3.353E-07	3.79E-01	1.26E-02	4.40E-03	1.32E-02	0	0.06	2.195	2000	1.20E-06
Pr-144	1.203E-05	3.30E-05	1.26E-02	4.40E-03	1.32E-02	0	8	0.467	1	0.00E+00
Pt-190	5.290E-08	6.50E+11	1.26E-02	4.40E-03	1.32E-02	0	5	0.305	2000	1.20E-06
Pt-193	3.732E-06	5.00E+01								3.10E-11
Pu-236	1.212E-10	2.86E+00	1.26E-02	4.40E-03	1.32E-02	0	63	3.724	9.10E-04	8.70E-08
Pu-238	7.618E-05	8.77E+01								2.30E-07
Pu-239	3.438E-02	2.41E+04								2.50E-07
Pu-240	1.689E-02	6.56E+03								2.50E-07
Pu-241	3.678E-03	1.43E+01								4.80E-09
Pu-242	1.318E-03	3.74E+05								2.40E-07
Pu-244	1.694E-19	8.11E+07								2.41E-07
Pu-246	1.901E-26	2.97E-02								3.33E-09
Ra-223	1.651E-15	3.13E-02								1.12E-02
Ra-224	5.035E-13	1.00E-02	7.13E-08							
Ra-225	1.765E-15	4.08E-02	9.90E-08							
Ra-226	1.397E-14	1.60E+03	2.80E-07							
Ra-228	3.296E-13	5.75E+00	6.90E-07							
Rb-87	1.691E-01	4.81E+10	1.26E-02	4.40E-03	1.32E-02	0	0.092	0.2305	2000	1.50E-09
Re-187	5.120E-04	4.33E+10	1.26E-02	4.40E-03	1.32E-02	0	63	0.051	2000	5.10E-12
Rh-102	1.593E-08	5.68E-01	1.26E-02	4.40E-03	1.32E-02	0	0	0.1923	2000	2.60E-09
Rh-106	2.001E-07	9.54E-07								0.00E+00
Rn-222	8.905E-20	1.05E-02	1.26E-02	4.40E-03	1.32E-02	0	0	0	2000	2.50E-10
Ru-106	1.695E-01	1.02E+00	1.26E-02	4.40E-03	1.32E-02	0	0	0.4835	2000	7.00E-09
S-35	4.591E-06	2.40E-01	1.26E-02	4.40E-03	1.32E-02	0	0	0.0493	2000	7.70E-10
Sb-124	1.355E-05	1.65E-01	1.26E-02	4.40E-03	1.32E-02	0	0.0045	0.2025	0.57	2.50E-09

Radionuclide	Inventory <sup>1</sup> [kg]	Half Life <sup>2</sup> [a]	Effective Diffusion Coefficient [m <sup>2</sup> /a]			Sorption Coefficient [m <sup>3</sup> /kg]			Solubility <sup>9</sup> [mol/m <sup>3</sup> ]	Dose Coefficient <sup>10</sup> [Sv/Bq]
			Gravel <sup>3</sup>	Clay <sup>4</sup>	Attenuation <sup>5</sup>	Gravel <sup>6</sup>	Clay <sup>7</sup>	Attenuation <sup>8</sup>		
Sb-125	5.506E-03	2.76E+00								1.10E-09
Sb-126	5.904E-06	3.38E-02								2.40E-09
Sc-46	8.550E-04	2.29E-01	1.26E-02	4.40E-03	1.32E-02	0	8	0.6087	2000	1.50E-09
Se-75	2.212E-05	3.28E-01	1.26E-02	4.40E-03	1.32E-02	0	0	0.631	1.26E-04	2.60E-09
Se-79	4.161E-03	2.95E+05								2.90E-09
Si-32	5.708E-12	1.53E+02	1.26E-02	4.40E-03	1.32E-02	0	0	0.1515	500	5.60E-10
Sm-145	2.317E-08	9.31E-01	1.26E-02	4.40E-03	1.32E-02	0	8	1.0945	0.024	2.10E-10
Sm-146	2.005E-07	1.03E+08								5.40E-08
Sm-147	1.861E-02	1.06E+11								4.90E-08
Sm-148	2.162E-02	7.00E+15								1.20E-06
Sm-151	4.051E-03	9.00E+01								9.80E-11
Sn-113	3.543E-08	3.15E-01	1.26E-02	4.40E-03	1.32E-02	0	63	0.572	9.63E-03	7.58E-10
Sn-119m	7.887E-06	8.02E-01								3.40E-10
Sn-121	1.208E-05	3.08E-03								2.30E-10
Sn-121m	2.926E-05	4.39E+01								3.80E-10
Sn-123	9.484E-05	3.54E-01								2.10E-09
Sn-126	1.227E-02	2.30E+05								4.74E-09
Sr-90	3.747E-01	2.88E+01	9.97E-03	4.40E-03	1.05E-02	0	0.0045	0.0823	5.5	2.80E-08
Ta-182	3.760E-05	3.14E-01	1.26E-02	4.40E-03	1.32E-02	0	3	1.042	2000	1.50E-09
Tb-157	3.338E-08	7.10E+01	1.26E-02	4.40E-03	1.32E-02	0	8	0.4455	2000	3.40E-11
Tb-160	2.445E-05	1.98E-01								1.60E-09
Tc-97	1.418E-07	4.21E+06	1.26E-02	4.40E-03	1.32E-02	0	63	0.000874	4.10E-05	6.80E-11
Tc-97m	1.765E-11	2.49E-01								5.50E-10
Tc-98	2.297E-07	4.20E+06								2.00E-09
Tc-99	5.639E-01	2.11E+05								6.40E-10
Te-121	2.448E-10	5.25E-02								1.26E-02
Te-121m	2.735E-10	4.50E-01	2.30E-09							

Radionuclide	Inventory <sup>1</sup> [kg]	Half Life <sup>2</sup> [a]	Effective Diffusion Coefficient [m <sup>2</sup> /a]			Sorption Coefficient [m <sup>3</sup> /kg]			Solubility <sup>9</sup> [mol/m <sup>3</sup> ]	Dose Coefficient <sup>10</sup> [Sv/Bq]
			Gravel <sup>3</sup>	Clay <sup>4</sup>	Attenuation <sup>5</sup>	Gravel <sup>6</sup>	Clay <sup>7</sup>	Attenuation <sup>8</sup>		
Te-123	1.690E-06	9.20E+16								4.40E-09
Te-123m	1.362E-07	3.26E-01								1.40E-09
Te-125m	5.613E-05	1.57E-01								8.70E-10
Te-127	4.694E-05	1.07E-03								0.00E+00
Te-127m	1.936E-03	2.99E-01								2.47E-09
Th-227	2.894E-15	5.11E-02								8.80E-09
Th-228	9.968E-11	1.91E+00								7.20E-08
Th-229	2.407E-10	7.34E+03								4.90E-07
Th-230	2.646E-09	7.54E+04	1.89E-03	4.40E-03	1.99E-03	0	63	4.74	2.49E-04	2.10E-07
Th-231	6.315E-10	2.91E-03								3.40E-10
Th-232	6.609E-03	1.40E+10								2.30E-07
Th-234	3.656E-09	6.60E-02								3.40E-09
Tl-204	4.804E-06	3.78E+00	1.26E-02	4.40E-03	1.32E-02	0	0	1.789	2000	1.20E-09
Tm-170	3.317E-05	3.52E-01	1.26E-02	4.40E-03	1.32E-02	0	8	1.07	2000	1.30E-09
Tm-171	8.029E-06	1.92E+00								1.10E-10
U-232	3.112E-08	6.89E+01								3.30E-07
U-233	9.476E-05	1.59E+05								5.10E-08
U-234	5.688E-04	2.45E+05								4.90E-08
U-235	2.242E-02	7.04E+08	1.26E-02	4.40E-03	1.32E-02	0	63	0.1742	3.45E-05	4.70E-08
U-236	1.099E-02	2.34E+07								4.70E-08
U-237	1.827E-05	1.85E-02								7.60E-10
U-238	1.301E+01	4.47E+09								4.50E-08
V-50	9.101E-05	1.40E+17	1.26E-02	4.40E-03	1.32E-02	0	0.0045	1.533	2000	1.20E-06
W-181	2.030E-07	3.32E-01								7.60E-11
W-185	3.590E-06	2.06E-01	1.26E-02	4.40E-03	1.32E-02	0	0.089	0.46	2000	4.40E-10
W-188	2.022E-07	1.91E-01								3.50E-09
Y-90	1.057E-04	7.30E-03	1.26E-02	4.40E-03	1.32E-02	0	8	0.861	2000	2.70E-09

Radionuclide	Inventory <sup>1</sup> [kg]	Half Life <sup>2</sup> [a]	Effective Diffusion Coefficient [m <sup>2</sup> /a]			Sorption Coefficient [m <sup>3</sup> /kg]			Solubility <sup>9</sup> [mol/m <sup>3</sup> ]	Dose Coefficient <sup>10</sup> [Sv/Bq]
			Gravel <sup>3</sup>	Clay <sup>4</sup>	Attenuation <sup>5</sup>	Gravel <sup>6</sup>	Clay <sup>7</sup>	Attenuation <sup>8</sup>		
Y-91	7.402E-02	1.60E-01								2.40E-09
Zn-65	2.072E-05	6.68E-01	1.26E-02	4.40E-03	1.32E-02	0	0.0045	1.96	2000	3.90E-09
Zr-93	3.227E-01	1.53E+06	1.26E-02	4.40E-03	1.32E-02	0	4	2.81	1.82E-04	1.10E-09
Zr-95	1.190E-01	1.75E-01								9.50E-10

<sup>1</sup>Based on inventory data from Tait et al. 2002 and assumptions in Section 2.4.

<sup>2</sup>Half-life data from ENDF/B-VII.1 (Chadwick et al. 2011).

<sup>3</sup>Gravel effective diffusion coefficient based on free water diffusion coefficient from Ohlsson and Neretnieks (1997), porosity of 0.4 (Section 5.2.2.4) and an assumed tortuosity of 1.

<sup>4</sup>Clay effective diffusion coefficient assumed to be value of neutral species from the SR-Site data report (SKB TR-10-52) as in Garisto et al. (2012).

<sup>5</sup>Attenuation layer effective diffusion coefficient based on free water diffusion coefficient from Ohlsson and Neretnieks (1997), porosity of 0.42 (Section 5.2.2.4) and an assumed tortuosity of 1.

<sup>6</sup>Gravel K<sub>d</sub> assumed to be zero for all species.

<sup>7</sup>Clay K<sub>d</sub> data assumed to be the same as bentonite in crystalline rock from Gobien and Garisto (2012).

<sup>8</sup>Attenuation layer K<sub>d</sub> data assumed to be the same as overburden (10% sand, 20% silt and 70% clay) from Gobien and Garisto (2012).

<sup>9</sup>Solubility data from Gobien and Garisto (2012).

<sup>10</sup>Ingestion dose coefficient from Gobien and Garisto (2012).

## APPENDIX B – AMBER MODEL THEORY

AMBER was selected as a platform to develop the landfill postclosure assessment model. AMBER is a compartment model that allows users to defined transfer rates between compartments, can model a large number of radioactive species, and accounts for radioactive decay and ingrowth and (Quintessa, 2013).

### B.1 COMPARTMENT MODELLING

Mathematically, the amount of a given radionuclide in any compartment is determined by Equation (1) (Quintessa, 2013). If the total amount (moles) of radionuclide  $m$  in compartment  $i$  is  $A_i^m$  then this satisfies:

$$\frac{dA_i^m}{dt} = - \left[ \lambda_r^m + \sum_j \lambda_{ij} \right] A_i^m + \lambda_r^{m+1} A_i^{m+1} + \sum_j \lambda_{ji} A_j^m \quad (1)$$

Where  $\lambda_{ij}$  is the exchange rate between compartment  $i$  and compartment  $j$  [in 1/a], conversely  $\lambda_{ji}$  is the exchange rate between compartment  $j$  and compartment  $i$  [in 1/a],  $\lambda_r^m$  is the decay rate of radionuclide  $m$  [in 1/a] and  $\lambda_r^{m+1}$  is the decay rate of the parent radionuclide  $m+1$  [in 1/a].

$A_i^{m+1}$  is the amount of the parent radionuclide in compartment  $i$  [in mol] and  $A_j^m$  is the amount of nuclide  $m$  in compartment  $j$  [in mol].

### B.2 WASTEFORM DEGRADATION

The loss rate of radionuclides in the wastefrom are described by equation (2)

$$\lambda_{deg} = \frac{R_{deg} A_{surface}}{M_{wasteform}} \quad (2)$$

Where  $\lambda_{deg}$  is the mass loss rate due to leaching or degradation of the wastefrom from the compartment representing the fast reactor wastefrom,  $R_{deg}$  is the elemental leaching rate or the wastefrom degradation rate (in kg/m<sup>2</sup>/a),  $A_{surface}$  is the surface are of the fast reactor wastefrom (in m<sup>2</sup>) and  $M_{wasteform}$  is the mass of the fast reactor wastefrom (in kg). In the case of the congruent release from the wastefrom the loss of an individual species is calculated by multiplying the degradation rate by the fractional inventory of a given species.

### B.3 ADVECTIVE AND DIFFUSIVE TRANSPORT

Advective transport in the compartment model can be modelled using equation (3)

$$\lambda_{adv}^m = \frac{v}{d\theta R^m} \quad (3)$$

where,  $\lambda_{adv}$  is the advective transfer rate from one compartment to the next,  $v$ , is the velocity (in m/a),  $d$  is the transport distance,  $\theta$  is the porosity of the layer and  $R$  is the retardation factor for a given radionuclide  $m$  described by equation (4).

$$R^m = 1 + \frac{\rho K_d^m}{\theta} \quad (4)$$

In equation (4),  $\rho$  is the density of a given layer and  $K_d^m$  is the sorption coefficient for a given radionuclide.

To model dispersion, a series of compartments are used to adjust the numerical dispersion resulting from the compartment model approach to that of the actual advective dispersion in the system. The Peclet Number is used as an indication of whether or not the numerical dispersion accurately captures the actual dispersion. Equation (5) shows the relationship between the Peclet number, dispersion length and the number of compartments.

$$P_e = \frac{d}{\alpha} = 2N \quad (5)$$

Where  $P_e$  is the Peclet Number,  $d$  is the transport length,  $\alpha$  is the dispersion length and  $N$  is the number of compartments used to represent the transport length. In this assessment, five compartments are used to represent each layer which corresponds to a dispersion length of 10% of the transport length.

Diffusive transport is modelled as both a forward and backward component from one compartment to the next. Equation (6) and (7) describe diffusive transport rate for the forward component ( $\lambda_{diff,fwd}$ ) from a given compartment and backward component ( $\lambda_{diff,bwd}$ ) from the following compartment.

$$\lambda_{diff,fwd}^m = \frac{D_{eff,1}^m}{d_1^2 \theta_1 R_1^m} \quad (6)$$

$$\lambda_{diff,bwd}^m = \frac{D_{eff,2}^m}{d_2^2 \theta_2 R_2^m} \quad (7)$$

Where  $D_{eff,1}$  and  $D_{eff,2}$  are the effective diffusion coefficient in the first and second compartments respectively. Similarly,  $d_1$ ,  $d_2$ ,  $\theta_1$ ,  $\theta_2$ ,  $R_1$  and  $R_2$  are the transport length, porosity and retardation of the two compartments respectively.

#### B.4 DOSE PATHWAYS

As previously mentioned the only dose pathway considered is drinking contaminated well water that draws on the aquifer near the landfill site. Equation (8) describes the well water concentration,  $C_{well}$ , in mol/m<sup>3</sup>.

$$C_{well}^m = \frac{A_{A\ aquifer}^m \lambda_{aquifer}^m f_{well}}{Q_{well}} \quad (8)$$

Where  $A_{A\ aquifer}^m$  is the amount (in moles) of radionuclide  $m$  in the aquifer compartment,  $f_{well}$  is the well capture fraction,  $Q_{well}$  is the well demand (in  $m^3/a$ ) and  $\lambda_{aquifer}$  is the advective transport rate (in  $1/a$ ) in the aquifer given by equation (3). The resulting total dose from drinking the contaminated well water ( $D_{well}$  in  $Sv/a$ ) is given by equation (9)

$$D_{well} = \sum_m C_{well}^m I_{wtr} f_{mol-bq}^m DC_{ing}^m \quad (9)$$

Where  $I_{wtr}$  is the water ingestion rate (in  $m^3/a$ ),  $f_{mol-bq}$  is the conversion factor from mol to bq for a given radionuclide (in  $Bq/mol$ ) and  $DC_{ing}$  is the dose conversion factor for the ingestion of a given radionuclide (in  $Sv/Bq$ ).